Computer Vision and Image Understanding 000 (2017) 1–15

Contents lists available at ScienceDirect

Computer Vision and Image Understanding

journal homepage: www.elsevier.com/locate/cviu

Ultimate levelings

Wonder A.L. Alves[a,b], Ronaldo F. Hashimoto[b,*], Beatriz Marcotegui[c]

[a] Informatics and Knowledge Management Graduate Program, Universidade Nove de Julho, São Paulo, Brazil
[b] Department of Computer Science, Institute of Mathematics and Statistics, Universidade de São Paulo, São Paulo, Brazil
[c] Centre for Mathematical Morphology, Mines-ParisTech, Fontainebleau, France

ARTICLE INFO

Article history:
Received 21 September 2016
Revised 16 April 2017
Accepted 27 June 2017
Available online xxx

Keywords:
Residual morphological operator
Ultimate attribute openings
Ultimate grain filters
Levelings
Component trees
Tree of shapes

ABSTRACT

This work presents a new class of residual operators called ultimate levelings which are powerful image operators based on numerical residues. Within a multi-scale framework, these operators analyze a given image under a series of levelings. Thus, contrasted objects can be detected if a relevant residue is generated when they are filtered out by one of these levelings. Our approach consists of, firstly, (*i*) representing the input image as a morphological tree; then, (*ii*) showing that a certain operation on this tree results in a leveling operator; and finally (*iii*) demonstrating that a sequential application of this operation on the tree is able to produce a family of levelings that satisfies scale-space properties. Besides, other contributions of this paper include: (*i*) the statement of properties of ultimate levelings, (*ii*) the presentation of an efficient algorithm for their computation, (*iii*) the provision of strategies for choosing families of primitives, (*iv*) the presentation of strategies for filtering undesirable residues, and (*v*) the provision of some illustrative examples of application of ultimate levelings. Furthermore, ultimate levelings are computationally efficient and their performance evaluations are comparable to the state of art methods for filtering and image segmentation.

1. Introduction

An operator in Mathematical Morphology (MM) can be seen as a mapping between complete lattices (Serra, 1988). In particular, mappings on the set of all gray level images $\mathcal{F}(\mathcal{D})$ defined on domain $\mathcal{D} \subset \mathbb{Z}^2$ and co-domain $\mathbb{K} = \{0, 1, \ldots, K\}$ are of special interest in MM, i.e., $\psi : \mathcal{F}(\mathcal{D}) \to \mathcal{F}(\mathcal{D})$. Furthermore, when ψ satisfies the properties of being increasing ($\forall f, g \in \mathcal{F}(\mathcal{D}), f \leq g \iff \psi(f) \leq \psi(g)$) and idempotent ($\forall f \in \mathcal{F}(\mathcal{D}), \psi(f) = \psi(\psi(f))$), it is called *morphological filter* (Serra, 1988). The first condition preserves the lattice relation order, while the second condition responds to the fact that increasing operations are not invertible. By using these properties, information content reductions are expected after applying morphological filters (Serra and Vincent, 1992). Relying on these characteristics, morphological filters remove selectively undesirable contents from images such as noise, background irregularities, etc.; while preserving desired contents (Bangham et al., 1996a, 1996b; Najman and Talbot, 2013). However, this is not always an easy task.

A complementary strategy is to effectively erase the desirable portion of an image, and then restore it through a difference with the original image. This gives rise to the idea of *residual operators*. Simply put, residual operators are transformations that involve combinations of morphological operators with differences (or subtractions). Morphological gradient, top-hat transforms, skeleton by maximal balls, ultimate erosion and ultimate opening are some examples of residual operators widely used in image processing applications.

In this study, we present a new large class of residual operators based on an indexed family of levelings. This class of residual operators analyzes the evolution of the residual value between two consecutive operators on a scale-space of levelings. The residual value of these operators can reveal important contrast information in images. This new class of operators includes some existing ones such as maximum difference of openings (resp., closings) by reconstruction (Li et al., 1997), differential morphological profiles (Pesaresi and Benediktsson, 2000), ultimate attribute openings (resp., closings) (Retornaz and Marcotegui, 2007), differential attribute profiles (Dalla Mura et al., 2010), shape ultimate attribute openings (resp., closings) (Hernández and Marcotegui, 2011) and ultimate grain filters (Alves and Hashimoto, 2014). They have successfully been used as a preprocessing step in various applications such as texture features extraction (Li et al., 1997), segmentation of high-resolution satellite imagery (Dalla Mura et al., 2010; Pesaresi and Benediktsson, 2001), text location (Alves and Hashimoto, 2010; Retornaz and Marcotegui, 2007), segmentation of building

* Corresponding author.
E-mail addresses: wonder@uni9.pro.br (W.A.L. Alves), ronaldo@ime.usp.br (R.F. Hashimoto), beatriz.marcotegui@mines-paristech.fr (B. Marcotegui).

http://dx.doi.org/10.1016/j.cviu.2017.06.010
1077-3142/

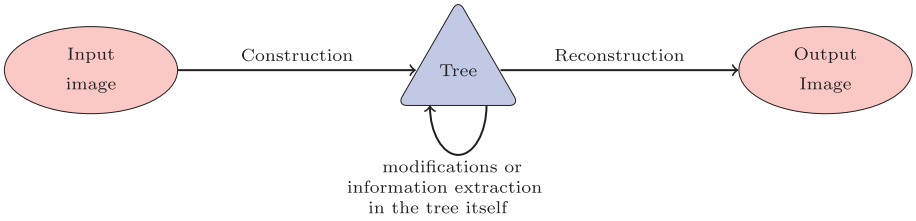

Fig. 1. Image representation through a tree.

façades (Hernández and Marcotegui, 2011) and restoration of historical documents (Meyer, 2010). Given above considerations, in this paper, besides the presentation of this new class of residual operators, which we call *ultimate levelings*, we also show its properties, fast algorithms for its computation and possible applications for residual information extraction in image processing applications.

The remainder of this paper is structured as follows. Section 2 briefly recall some definitions and properties about scale-space representations based on levelings and residual operators. In Section 3, we provide the main contributions of this paper by (*i*) introducing the ultimate leveling as a class of residual operators, (*ii*) stating some of its properties and (*iii*) presenting an efficient algorithm for its computation. Section 4 provides some strategies for choosing a family of primitives. In Section 5, we present some strategies for filtering undesirable residues and, Section 6 provides some illustrative examples of application of ultimate levelings. Finally, Section 7 concludes this work and presents some future research directions.

2. Theoretical background

In many image processing problems, objects of interest may be present at different scales. For such situations, multi-scale approaches have been developed over the last few decades, where a sequence of coarser and coarser decompositions of the same image are derived. In this sense, Meyer and Maragos (2000) proposed a nonlinear scale-space (sequence of images) decomposition obtained from a sequence of operators of a general class of morphological filters called levelings giving rise to *morphological scale-space based on levelings*. Later, Alves et al. (2015) proved that there exists an efficient representation of morphological scale-space based on levelings through hierarchies of level sets.

Thus, for the sake of understanding, Sections 2.1 and 2.2 recall some definitions and properties of hierarchies of level sets and morphological scale-space based on levelings, respectively. Then, we present an efficient representation of morphological scale-spaces based on levelings through hierarchies of level sets. And, Section 2.3 provides a link between the state of art in residual operators and the main result of this paper, given in Section 3.

2.1. Hierarchies of level sets: component tree and tree of shapes

Image representations through trees have been proposed in recent years to carry out tasks of image processing and analysis such as filtering, segmentation, pattern recognition, contrast extraction, registration, compression and others. In this scenario, as illustrated in Fig. 1, the first step consists of constructing a representation of the input image by means of a tree, then the task of image processing or analysis is performed through modifications or information extraction in the tree itself, and finally an image is reconstructed from the modified tree.

In order to build the trees considered in this paper, we need the following definitions. For any $\lambda \in \mathbb{K} = \{0, 1, \ldots, K\}$, we define $\mathcal{X}^{\lambda}_{\downarrow}(f) = \{p \in \mathcal{D} : f(p) < \lambda\}$ and $\mathcal{X}^{\uparrow}_{\lambda}(f) = \{p \in \mathcal{D} : f(p) \geq \lambda\}$ as the *lower* and *upper level sets* at value λ from an image $f \in \mathcal{F}(\mathcal{D})$, respectively. These level sets are nested, i.e., $\mathcal{X}^{1}_{\downarrow}(f) \subseteq \mathcal{X}^{2}_{\downarrow}(f) \subseteq \ldots \subseteq \mathcal{X}^{K}_{\downarrow}(f)$ and $\mathcal{X}^{\uparrow}_{K}(f) \subseteq \mathcal{X}^{\uparrow}_{K-1}(f) \subseteq \ldots \subseteq \mathcal{X}^{\uparrow}_{0}(f)$. It is possible to show that the image f can be reconstructed using either the family of lower or upper sets, i.e., $\forall p \in \mathcal{D}$,

$$f(p) = \sup\{\lambda : p \in \mathcal{X}^{\uparrow}_{\lambda}(f)\} = \inf\{\lambda - 1 : p \in \mathcal{X}^{\lambda}_{\downarrow}(f)\}. \quad (1)$$

Examples of lower and upper level sets are presented in Fig. 2. Observe that, given a $\lambda \in \mathbb{K}$, the level set $\mathcal{X}^{\lambda}_{\downarrow}(f)$ or $\mathcal{X}^{\uparrow}_{\lambda}(f)$ may have more than one connected component.

From lower or upper level sets, we define two other sets $\mathcal{L}(f)$ and $\mathcal{U}(f)$ composed by the connected components (CCs) of the lower and upper level sets of f, i.e., $\mathcal{L}(f) = \{C \in \mathcal{CC}_4(\mathcal{X}^{\lambda}_{\downarrow}(f)) : \lambda \in \mathbb{K}\}$ and $\mathcal{U}(f) = \{C \in \mathcal{CC}_8(\mathcal{X}^{\uparrow}_{\lambda}(f)) : \lambda \in \mathbb{K}\}$, where $\mathcal{CC}_4(X)$ and $\mathcal{CC}_8(X)$ are sets of 4 and 8 connected CCs of X, respectively. The ordered pairs consisting of the CCs of the lower and upper level sets and the usual inclusion set relation, i.e., $(\mathcal{L}(f), \subseteq)$ and $(\mathcal{U}(f), \subseteq)$, induce two dual trees (Caselles et al., 2008) called *component trees*. This leads us to Definition 2.1, and consequently to Proposition 2.2. In Fig. 3, we have examples of component trees $(\mathcal{L}(f), \subseteq)$ and $(\mathcal{U}(f), \subseteq)$ built from the lower and upper level sets presented in Fig. 2. Observe that the CCs of the lower or upper level sets extracted from an image have a hierarchical structure in these trees.

Definition 2.1. Let $(\mathcal{T}, \preceq)$ be an ordered set. We say that $\preceq$ induces a tree structure in $\mathcal{T}$ if the following two conditions hold:

1. $\exists R \in \mathcal{T}$ such that $\forall N \in \mathcal{T}, N \preceq R$. In that case we shall say that R is the root of the tree.
2. $\forall A, B, C \in \mathcal{T}$, if $A \preceq B$ and $A \preceq C$ then either $B \preceq C$ or $C \preceq B$. In that case, we shall say that B and C are nested.

Proposition 2.2. (Caselles et al.(2008)) *Both* $(\mathcal{L}(f), \subseteq)$ *and* $(\mathcal{U}(f), \subseteq)$ *are trees.*

2.1.1. Tree of shapes

Combining these dual trees $(\mathcal{L}(f), \subseteq)$ and $(\mathcal{U}(f), \subseteq)$ into a single tree, the so called *tree of shapes* can be built (Caselles et al., 2008; Monasse and Guichard, 2000). In fact, let $\mathcal{P}(\mathcal{D})$ denote the *powerset* of $\mathcal{D}$ and let $sat : \mathcal{P}(\mathcal{D}) \to \mathcal{P}(\mathcal{D})$ be the operator of saturation (Caselles et al., 2008; Caselles and Monasse, 2010; Monasse and Guichard, 2000). Thus, let $\mathcal{SAT}(f) = \{sat(C) : C \in \mathcal{L}(f) \cup \mathcal{U}(f)\}$ be the family of CCs of the lower and upper level sets, respectively, with all holes filled. The elements of $\mathcal{SAT}(f)$, called *shapes*, are nested by the inclusion relation. The pair $(\mathcal{SAT}(f), \subseteq)$ induces a tree (see Proposition 2.3) which is called *tree of shapes* (Caselles et al., 2008; Caselles and Monasse, 2010). Fig. 3, we have an example of tree of shapes $(\mathcal{SAT}(f), \subseteq)$ built from the lower and upper level sets presented in Fig. 2.

Proposition 2.3. (Caselles et al.(2008)) *The ordered set* $(\mathcal{SAT}(f), \subseteq)$ *is a tree.*

2.1.2. Compact representation of trees

Tree of shapes and also component trees of an image f will be denoted generically by $\mathcal{T}_f$. It is well known that a tree $\mathcal{T}_f$

Please cite this article as: W.A.L. Alves et al., Ultimate levelings, Computer Vision and Image Understanding (2017), http://dx.doi.org/10.1016/j.cviu.2017.06.010

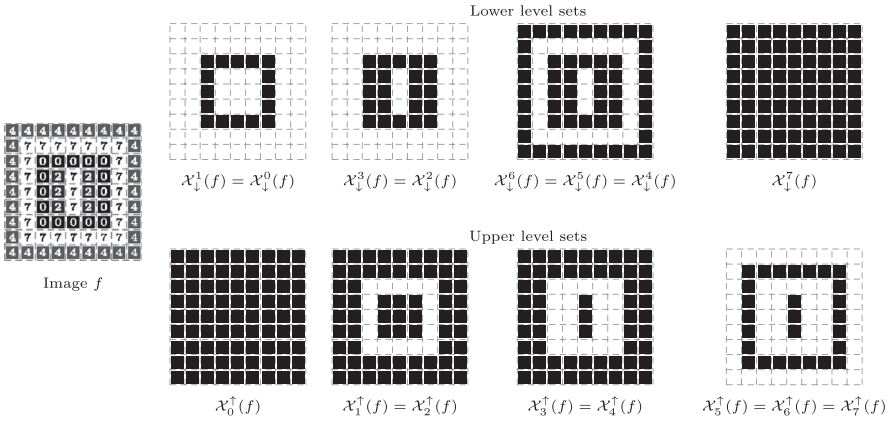

Fig. 2. Examples of lower and upper level sets extracted from an image. At right is the input image f and at top and bottom rows, respectively, are the level sets $\mathcal{X}^\lambda_\downarrow(f)$ and $\mathcal{X}^\uparrow_\lambda(f)$.

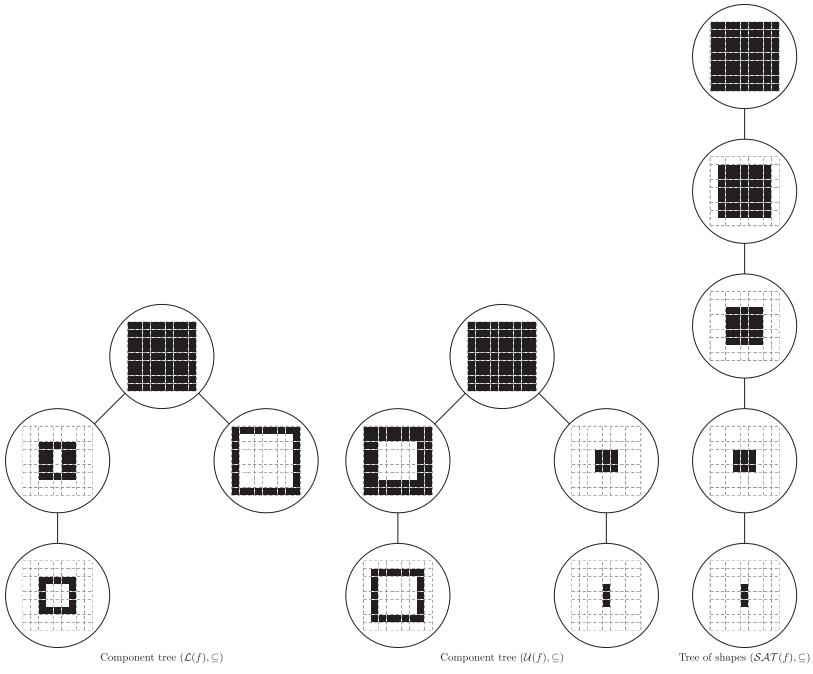

Fig. 3. Examples of trees $(\mathcal{L}(f), \subseteq)$ and $(\mathcal{U}(f), \subseteq)$ built from the lower and upper level sets presented in Fig. 2.

can be completely represented by a compact and non-redundant data structure (Caselles and Monasse, 2010; Géraud et al., 2013) so that, for each pixel $p \in \mathcal{D}$ is associated to the smallest shape or CC of the tree containing p. In this structure, by the parenthood relationship, one can easily find that, all its ancestors shapes or CCs in the tree are also associated to this pixel p. Then, we denote by $\mathcal{SC}(\mathcal{T}_f, p)$ the smallest shape or CC containing p in the tree $\mathcal{T}_f$. In particular, the compact representations of component trees $(\mathcal{L}(f), \subseteq)$ and $(\mathcal{U}(f), \subseteq)$ are known as, respectively, *min-tree* and *max-tree* (Carlinet and Géraud, 2013; Salembier et al., 1998). Fig. 4 shows the component trees of Fig. 3 along with the highlighted pixels in red indicating their smallest component.

2.1.3. Image reconstruction from trees

Note that, by definition, an image can be reconstructed from its level sets (see Eq. (1)). Inspired by this equation, we can define mappings $level_\mathcal{L} : \mathcal{L}(f) \to \mathbb{K}$, $level_\mathcal{U} : \mathcal{U}(f) \to \mathbb{K}$ and $level_{\mathcal{SAT}} : \mathcal{SAT}(f) \to \mathbb{K}$ as follows:

$$\begin{aligned} &level_\mathcal{L}(C) = \inf\{\lambda - 1 : C \in \mathcal{CC}_4(\mathcal{X}^\lambda_\downarrow(f)), \lambda \in \mathbb{K}\},\\ &level_\mathcal{U}(C) = \sup\{\lambda : C \in \mathcal{CC}_8(\mathcal{X}^\uparrow_\lambda(f)), \lambda \in \mathbb{K}\} \text{ and}\\ &level_{\mathcal{SAT}}(C) = f(y) \text{ such that } y \in \arg\sup\{|\mathcal{SC}(\mathcal{T}_f, x)| : x \in C\},\\ &\text{where} \mathcal{T}_f = (\mathcal{SAT}(f), \subseteq). \end{aligned} \tag{2}$$

For the sake of simpler notation, from now on, the subscript indicating the tree will be dropped from the mappings *level* when it is clear from context. Using the mapping *level*, it is possible to prove that an image $f \in \mathcal{F}(\mathcal{D})$ can be reconstructed from a tree $\mathcal{T}_f$ as follows, $\forall p \in \mathcal{D}, f(p) = level(\mathcal{SC}(\mathcal{T}_f, p))$. In such a case, we write: $f = Rec(\mathcal{T}_f)$. In particular, if f is obtained by $Rec((\mathcal{L}(f), \subseteq))$ (resp., $Rec((\mathcal{U}(f), \subseteq))$ and $Rec((\mathcal{SAT}(f), \subseteq))$), then this operation is called *lower* (resp., *upper* and *shape*) *reconstruction*.

2.1.4. Pruning operations

Now, the following definition (Definition 2.4) characterizes *pruning operations* of a tree $(\mathcal{T}, \preceq)$.

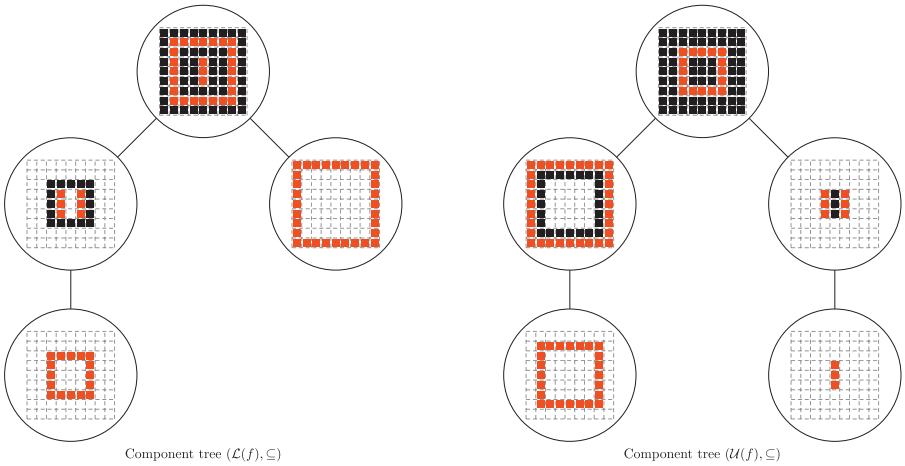

Fig. 4. Examples of component trees along with the highlighted pixels in red indicating their smallest component. (For interpretation of the references to color in this figure legend, the reader is referred to the web version of this article.)

Definition 2.4. We say that $(\mathcal{T}', \preceq)$ is obtained by a pruning operation of a tree $(\mathcal{T}, \preceq)$ if and only if, $\mathcal{T}' \subseteq \mathcal{T}$, for any $X \in \mathcal{T}'$, $\nexists Y \in (\mathcal{T} \setminus \mathcal{T}')$ such that $X \preceq Y$. In such a case, we write $\mathcal{T}' = \mathcal{P}_{runing}(\mathcal{T})$.

Following this definition, if $\mathcal{T}_f$ is a tree of an image $f \in \mathcal{F}(\mathcal{D})$, then we say $\mathcal{T}_g$ is the pruned version of $\mathcal{T}_f$ if and only if $\mathcal{T}_g = \mathcal{P}_{runing}(\mathcal{T}_f)$. Also, one can easily see that $\mathcal{T}_g \subseteq \mathcal{T}_f$ and $\mathcal{T}_g$ is still a tree (not a forest). In addition, since the nodes of $\mathcal{T}_f$ and $\mathcal{T}_g$ are nested by the inclusion relation order, it can be proved that, $\forall p \in \mathcal{D}$, $\mathcal{SC}(\mathcal{T}_f, p) \subseteq \mathcal{SC}(\mathcal{T}_g, p)$ (Alves et al., 2015).

At the end of this subsection, we have all the ingredients of Fig. 1, that is, given an input image f, construct a tree, followed by pruning operations that modifies the original tree, and, finally reconstructed the image from the modified tree.

2.2. Morphological scale-space based on levelings

As previously mentioned, in many applications in image processing, objects of interest in an image may belong to many scales. In this situation, several representations of scale-space have been developed in recent decades, such as the scale-space through levelings. In this sense, a scale-space based on levelings, which are specializations of connected operators, is presented in this section through a hierarchy of level sets, more specifically, through component trees and tree of shapes. For that, firstly we recall some theory on connected operators and levelings. Then, recall that reconstructions of pruned trees are levelings. Finally, recall that a tree represents a scale-space that can be constructed by successive pruning operations in the tree.

2.2.1. Connected operators and levelings

In a few words, a *connected operator* $\psi : \mathcal{F}(\mathcal{D}) \to \mathcal{F}(\mathcal{D})$ is a transformation that enlarges the partition of space created by flat zones and consequently do not create new contours (Salembier and Serra, 1995). More precisely, see Definition 2.5.

Definition 2.5 ([Salembier and Serra, 1995])**.** An operator $\psi : \mathcal{F}(\mathcal{D}) \to \mathcal{F}(\mathcal{D})$ is said to be *connected*, if and only if, for any $f \in \mathcal{F}(\mathcal{D})$ the following relation is valid for any pixel $p \in \mathcal{D}$, i. e.,

$$\mathbb{P}_f(p) \subseteq \mathbb{P}_{\psi(f)}(p),$$

where $\mathbb{P}_f$ and $\mathbb{P}_{\psi(f)}$ are two partitions on $\mathcal{D}$ generated by the flat zones of f and $\psi(f)$, respectively. In addition, $\mathbb{P}_f(p)$ and $\mathbb{P}_{\psi(f)}(p)$ are two regions of $\mathbb{P}_f$ and $\mathbb{P}_{\psi(f)}$ that contains the pixel p.

This definition emphasizes the processing based on regions since the output regions are obtained by merging adjacent regions from input image partition. An equivalent definition, introduced by Meyer (1998a), emphasizes the local processing of region contours, i.e., if there is a transition between two adjacent pixels (p, q) in the operator output (that is, $[\psi(f)](p) \neq [\psi(f)](q)$), then a transition also occurs between the same pixels in the input image (that is, $f(p) \neq f(q)$).

Connected operators represent a wide class of operators (Meyer, 1998b; 2004; Meyer and Maragos, 2000) extensively studied in the literature. One of these specializations, known as *levelings* (Meyer, 1998a; 1998b; 2004; Meyer and Maragos, 2000), is a powerful filter that preserves order, does not create new structures (regional extrema and contours) and its values are enclosed by values of neighbor pixels (see Definition 2.6).

Definition 2.6 ([Meyer (1998a, 1998b)])**.** An operator $\psi : \mathcal{F}(\mathcal{D}) \to \mathcal{F}(\mathcal{D})$ is said to be leveling, if and only if, for any $f \in \mathcal{F}(\mathcal{D})$ the following relation is valid for all pairs of adjacent pixels, i.e., $\forall (p, q) \in \mathcal{A}$,

$$[\psi(f)](p) > [\psi(f)](q) \Rightarrow f(p) \geq [\psi(f)](p) \text{ and } [\psi(f)](q) \geq f(q).$$

where $\mathcal{A}$ is a adjacency relation[1] on $\mathcal{D}$.

2.2.2. Morphological scale-space of levelings

Note that from the definition of a class of operators $\mathcal{C}$ (e.g., connected operators or levelings), it is possible to build a binary relation $\mathcal{R}$ on $\mathcal{F}(\mathcal{D})$ such that, for any $(g, f) \in \mathcal{R}$ if and only if there exists $\psi \in \mathcal{C}$ such that $g = \psi(f)$. Thus, definition of levelings can be seen as a binary relation $\mathcal{R}_{leveling}$ on $\mathcal{F}(\mathcal{D})$. Similarly, we can define the relation $\mathcal{R}_{connected}$. So, we say that g is leveling of f if and only if $(g, f) \in \mathcal{R}_{leveling}$. Analogously, g is connected of f if and only if $(g, f) \in \mathcal{R}_{connected}$. In Meyer (1998a), F. Meyer, shows that $\mathcal{R}_{leveling}$ is reflexive and transitive; and, if we ignore the constant images, then $\mathcal{R}_{leveling}$ is anti-symmetric, i.e., $\mathcal{R}_{leveling}$ is an order relation. With the help of this order relation, levelings can be nested and create a scale-space decomposition of an image $f \in \mathcal{F}(\mathcal{D})$ in the form of a series of levelings $(g_0 = f, g_1, \ldots, g_n)$, where g_k is leveling of g_{k-1} and, as a consequence of transitivity, g_k is also a leveling of each image g_j, for $j < k$ (Meyer and Maragos, 2000) and forms what we call a *morphological scale-space of levelings*.

Morphological scale-spaces are important for image segmentation since they have the following features: (i) simplification, i.e.,

[1] An adjacency relation $\mathcal{A}$ on $\mathcal{D}$ is binary relation on pixels of $\mathcal{D}$. Thus, $(p, q) \in \mathcal{A}$ if and only if p is an adjacent of q or alternatively $q \in \mathcal{A}(p)$. Common examples of adjacency relation on $\mathcal{D}$ are 4 or 8-connectivities.

Please cite this article as: W.A.L. Alves et al., Ultimate levelings, Computer Vision and Image Understanding (2017), http://dx.doi.org/10.1016/j.cviu.2017.06.010

Fig. 5. Example of a scale-space based on levelings.

all contours and all regional extrema of g_{i+1} are present in g_i; (*ii*) causality, i.e., any contour of g_{i+1} corresponds to a stronger contour of g_i at the same location; and (*iii*) fidelity, i.e., no new extrema at larger scales (Bangham et al., 1996a; 1996b; Meyer, 2010; Meyer and Maragos, 2000).

In Fig. 5, we have an example of morphological scale-space based on levelings. Observe that, the coarser is the scale, the more simplified is the image; and at larger scales there are neither new contours nor new extrema.

2.2.3. Reconstruction of pruned trees

In this way, Alves et al. (2015) showed that scale-spaces based on levelings can be obtained by successive sequences of prunings. More precisely, let $\mathcal{T}_f$ be a tree (max-tree, min-tree or tree of shapes) that represents an image $f \in \mathcal{F}(\mathcal{D})$ and let $(\mathcal{T}_f^0, \mathcal{T}_f^1, \mathcal{T}_f^2, \ldots)$ be a sequence of trees obtained by successive prunings, i.e.,

$$\mathcal{T}_f^i = \begin{cases} \mathcal{T}_f, & \text{if } i = 0, \\ \mathcal{P}runing(\mathcal{T}_f^{i-1}), & \text{if } i > 0. \end{cases} \qquad \text{for } i = 0, 1, 2, \ldots \quad (3)$$

Then, Alves et al. (2015) have proved that reconstructions from pruned trees are levelings. Hence, if $Rec(\mathcal{T}_f^n)$ is a leveling of $Rec(\mathcal{T}_f^k)$ and $Rec(\mathcal{T}_f^k)$ is a leveling of $Rec(\mathcal{T}_f^j)$, then, by transitivity, we have also that $Rec(\mathcal{T}_f^n)$ is a leveling of $Rec(\mathcal{T}_f^j)$, for any $0 \leq j \leq k \leq n$. This shows that the sequence of trees generates a family of levelings that subsequently simplifies the image f, thus constituting a morphological scale-space. This fact leads us to Theorem 2.7.

Theorem 2.7 ([Alves et al. (2015)])**.** *Let $\mathcal{T}_f$ be a tree (max-tree, min-tree or tree of shapes) that represents an image f. Let $(\mathcal{T}_f^0, \mathcal{T}_f^1, \ldots, \mathcal{T}_f^n)$ be a sequence of trees obtained by successive prunings. Then, the sequence of reconstructions $(Rec(\mathcal{T}_f^0), Rec(\mathcal{T}_f^1), \ldots, Rec(\mathcal{T}_f^n))$ is a morphological scale-space of levelings.*

2.3. Residual operators

This subsection provides a link between the state of art in residual operators and the main result of this paper, given in Section 3. As previously mentioned, a *residual operator* $r_{\psi,\phi} : \mathcal{F}(\mathcal{D}) \to \mathcal{F}(\mathcal{D})$ is defined as the difference between two operators, say $\psi : \mathcal{F}(\mathcal{D}) \to \mathcal{F}(\mathcal{D})$ and $\phi : \mathcal{F}(\mathcal{D}) \to \mathcal{F}(\mathcal{D})$, applied to a given image $f \in \mathcal{F}(\mathcal{D})$, i.e., $\forall p \in \mathcal{D}, [r_{\psi,\phi}(f)](p) = [\psi(f)](p) - [\phi(f)](p)$. Operators ψ and ϕ are called *primitives*, and if $[\psi(f)](p) > [\phi(f)](p)$, then we say $r_{\psi,\phi}(p)$ is a *positive residue*; or a *negative residue* if $[\psi(f)](p) < [\phi(f)](p)$; otherwise, we say $r_{\psi,\phi}(p)$ is a *null residue*. Residual operators have been extended to extract residues of two increasing families of primitives $\{\psi_i : \mathcal{F}(\mathcal{D}) \to \mathcal{F}(\mathcal{D}), i \in \mathcal{I}_\preccurlyeq\}$ and $\{\phi_i : \mathcal{F}(\mathcal{D}) \to \mathcal{F}(\mathcal{D}), i \in \mathcal{I}_\preccurlyeq\}$ indexed by a set $\mathcal{I}_\preccurlyeq = \{0, 1, \ldots, I_{MAX}\}$ such that, for any $i, j \in \mathcal{I}_\preccurlyeq$, if $i \leq j$, then $\psi_i \preccurlyeq \psi_j$ and $\phi_i \preccurlyeq \phi_j$. Note that, in notation of the index set $\mathcal{I}_\preccurlyeq$, it is explicitly indicated the partial order relation $\preccurlyeq$ between primitive operators. Thus, the ith residual operator applied to a given image $f \in \mathcal{F}(\mathcal{D})$ is defined as $r_{\psi_i,\phi_i}(f) = \psi_i(f) - \phi_i(f)$ and the extended residual operator $\theta : \mathcal{F}(\mathcal{D}) \to \mathcal{F}(\mathcal{D})$ applied to an image f is defined as the supremum of residues, i.e., $\theta(f) = \sup_{i \in \mathcal{I}_\preccurlyeq}\{r_{\psi_i,\phi_i}(f)\}$. Skeleton by maximal balls and ultimate erosion are examples of extended binary residual operators commonly used in binary image processing.

Some residual operators are defined on a single increasing family of primitives $\{\psi_i : i \in \mathcal{I}_\preccurlyeq\}$ such that $\psi_i \preccurlyeq \psi_{i+1}$ and residues $r_{\psi_i,\psi_{i+1}}$ are consecutively extracted along with the primitives family. For simplicity, we denote, from this moment on, the ith residual operator $r_{\psi_i,\psi_{i+1}}$ by r_i. Thus, in the same way as defined above, the *residual operator* defined from this single family is given by the supremum of consecutive residues applied for any image $f \in \mathcal{F}(\mathcal{D})$, that is,

$$\theta(f) = \sup_{i \in \mathcal{I}_\preccurlyeq}\{r_i(f) : r_i(f) = \psi_i(f) - \psi_{i+1}(f)\}. \quad (4)$$

In this sense, in 1997, Li et al. (1997) used the result of this operator, along with all the residues, when the primitives are openings (and by duality, closings) by reconstruction, to build, for each pixel $p \in \mathcal{D}$, features (among others) for texture classification.

A few years later, in 2000, Pesaresi and Benediktsson (2000), used the same concept to define, for each pixel $p \in \mathcal{D}$, the derivative of morphological profile applied to high resolution satellite images segmentation. The *morphological profile* is a large vector constructed, for each pixel $p \in \mathcal{D}$, by concatenation of openings (and by duality, closings) by reconstruction. The *derivative of morphological profile* is nothing more than the large vector built from all consecutive residues. Also in Pesaresi and Benediktsson (2000), the authors used, along with the derivative of morphological profile, the point where occurs its greatest derivative to build a large vector to characterize each pixel for image segmentation. It is worth mentioning that the studies initiated by Pesaresi and Benediktsson (2000; 2001) have had high-impact contributions in the remote sensing domain (Ghamisi et al., 2015).

Afterwards, in 2007, Beucher (2007) proposed the *ultimate opening* (and by duality, *ultimate closing*), which is a residual operator where the primitives are openings by structuring elements of increasing sizes $\{\gamma_{\mathcal{B}_i} : i \in \mathcal{I}_\geq\}$ (and, respectively, closings by structuring elements of decreasing sizes $\{\varphi_{\mathcal{B}_i} : i \in \mathcal{I}_\leq\}$). Many advances inspired in *morphological profile* and *ultimate opening* have been proposed over the last few years which include, for example, the *ultimate attribute opening* (UAO) and by duality *ultimate attribute closing* (UAC) (Retornaz and Marcotegui, 2007), which are residual operators where primitives are attribute openings $\{\gamma_i^\kappa : i \in \mathcal{I}_\geq\}$ and attribute closings $\{\varphi_i^\kappa : i \in \mathcal{I}_\leq\}$, respectively. Similarly, in Dalla Mura et al. (2010); Ouzounis et al. (2012), the authors have been proposed the attribute openings (resp. closings) profiles where the greatest derivatives are equivalent to the ultimate attribute opening based on the same primitives.

From the above, we can see that residual operators are very important for image processing and analysis.

2.3.1. Computation of residual operators by successive prunings

Algorithms for residual operator computation have been proposed using trees (Alves and Hashimoto, 2014; Fabrizio and Marcotegui, 2009; Ouzounis et al., 2012; Wilkinson et al., 2016; 2011). If $(\mathcal{T}_f^0, \mathcal{T}_f^1, \ldots, \mathcal{T}_f^{I_{MAX}})$ is a sequence of trees obtained by successive prunings from a tree $\mathcal{T}_f$ such that $\psi_0(f) = Rec(\mathcal{T}_f^0)$, $\psi_i(f) = Rec(\mathcal{T}_f^i)$ and $\mathcal{T}_f^i = \mathcal{P}runing(\mathcal{T}_f^{i-1})$, for $i \in \mathcal{I}$, then $(\psi_0(f), \psi_1(f), \ldots, \psi_{I_{MAX}}(f))$ constitutes a morphological scale-

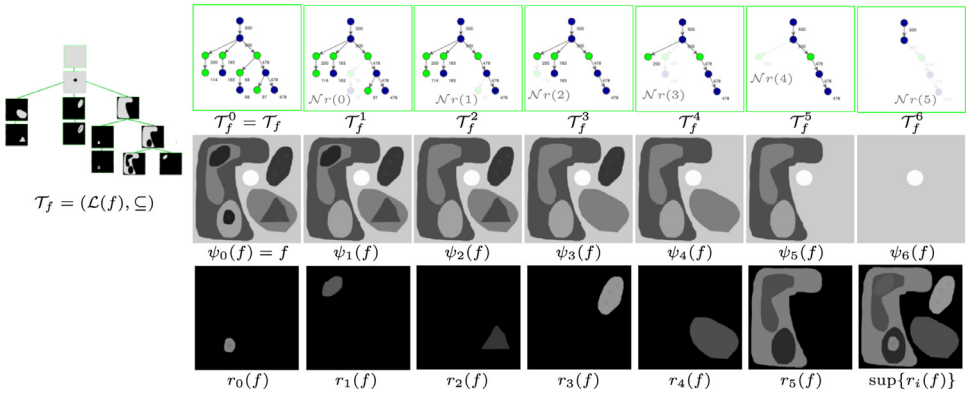

Fig. 6. An example of ultimate attribute closing is shown: (top) Trees derived by successive prunings; (middle) primitives family $\{\psi_i(f) : \psi_i(f) = Rec(\mathcal{T}_i), i = 0, 1, \ldots, 6\}$; (bottom) extracted residues $\{r_0(f), r_1(f), \ldots, r_5(f)\}$; and the result of ultimate attribute closing $\sup\{r_i(f)\}$.

space based on levelings. Then, the nodes of $\mathcal{T}_f^i$, which are not in $\mathcal{T}_f^{i+1}$, can be used to calculate the residues $r_i(f)$ between $\psi_i(f)$ and $\psi_{i+1}(f)$. In Fig. 6, we have an example of computation of the residual operator (at the bottom right) by a sequence of successive prunings (at the top row) of the component tree $(\mathcal{L}(f), \subseteq)$ (at left). Note that the morphological scale-space and residues are given, respectively, at the middle and bottom rows.

In this way, a consecutive residual operator can be obtained by a sequence of successive prunings of a tree which in turn defines a morphological scale-space based on specific family of levelings. In this paper, a larger collection of levelings is considered. The resulting operators are called *ultimate levelings* and they will be defined more formally in Section 3.

3. Ultimate levelings

Ultimate levelings constitute a wider class of residual operators defined from an indexed family of levelings $\{\psi_i : i \in \mathcal{I}\}$ such that for any $i, j \in \mathcal{I}$, $i \leq j \Leftrightarrow \psi_j$ is *leveling* of ψ_i. Note that this larger class of operator includes families of openings and closings by reconstruction studied by Pesaresi and Benediktsson (2000). An ultimate leveling analyzes the evolution of the residual value presented in two consecutive primitives, i.e. $r_i^+(f) = [\psi_i(f) - \psi_{i+1}(f) \vee 0]$ and $r_i^-(f) = [\psi_i(f) - \psi_{i+1}(f) \vee 0]$, keeping the maximum positive and negative residues for each pixel. More precisely, see Definition 3.1.

Definition 3.1 (Ultimate levelings)**.** A *positive ultimate leveling operator* $\mathcal{R}_\theta^+$ (resp., *negative* $\mathcal{R}_\theta^-$) is the supremum of positive (resp., negative) residues r_i^+ (resp., r_i^-) extracted from a family $\{\psi_i : i \in \mathcal{I}\}$ indexed by a set $\mathcal{I}$, such that, for any $i, j \in \mathcal{I}$, $i \leq j \Leftrightarrow \psi_j$ is a *leveling* of ψ_i. That is, $\mathcal{R}_\theta^+(f) = \sup_{i\in\mathcal{I}}\{r_i^+(f) : r_i^+(f) = [\psi_i(f) - \psi_{i+1}(f) \vee 0]\}$ (resp., $\mathcal{R}_\theta^-(f) = \sup_{i\in\mathcal{I}}\{r_i^-(f) : r_i^-(f) = [\psi_{i+1}(f) - \psi_i(f) \vee 0]\}$). Thus, the *ultimate leveling* $\mathcal{R}_\theta$ is the supremum between $\mathcal{R}_\theta^+$ and $\mathcal{R}_\theta^-$, i.e., $\mathcal{R}_\theta(f) = \mathcal{R}_\theta^+(f) \vee \mathcal{R}_\theta^-(f)$.

3.1. Associated information to ultimate levelings

Residual values of these operators can reveal important contrasted structures in the image. Besides residues, other associated information can be obtained such as properties of the operators that produced the residual value. For example, Beucher (2007) introduced a function $q_{\mathcal{I}_{\max}} : \mathcal{D} \to \mathcal{I}$ that associates to each pixel the major index that produces the maximum non-null residue, i.e.,

$$q_{\mathcal{I}_{\max}}^+(p) = \max\{i+1 : [r_i^+(f)](p) = [\mathcal{R}_\theta^+(f)](p) > 0\} \quad (5)$$

and

$$q_{\mathcal{I}_{\max}}^-(p) = \max\{i+1 : [r_i^-(f)](p) = [\mathcal{R}_\theta^-(f)](p) > 0\}. \quad (6)$$

The functions $q_{\mathcal{I}_{\max}}^+$ and $q_{\mathcal{I}_{\max}}^-$ (resp., $q_{\kappa_{\max}}^+$ and $q_{\kappa_{\max}}^-$) are combined into a single function $q_{\mathcal{I}_{\max}}$ (resp., $q_{\kappa_{\max}}$), i.e.,

$$p \in \mathcal{D}, q_{\mathcal{I}_{\max}}(p) = \begin{cases} q_{\mathcal{I}_{\max}}^+(p), & \text{if } [\mathcal{R}_\theta(f)](p) > [\mathcal{R}_\theta^+(f)](p), \\ q_{\mathcal{I}_{\max}}^-(p), & \text{otherwise.} \end{cases} \quad (7)$$

Furthermore, replacing the max operator by any other rank-order operators can have some other interesting functions as, for example: $q_{\mathcal{I}_{\text{median}}}$ $q_{\mathcal{I}_{\min}}$, $q_{\kappa_{\text{median}}}$ and $q_{\kappa_{\min}}$. These functions may be very useful to analyze the extracted residues as already done in some applications (Alves et al., 2013; Beucher, 2007; Hernández and Marcotegui, 2011; Pesaresi and Benediktsson, 2000; 2001).

In Fig. 7, we present the input image f (shown in Fig. 6), its ultimate leveling $\mathcal{R}_\theta(f)$, and the associated image $q_{\mathcal{I}_{\max}}$. Note that the colors in $q_{\mathcal{I}_{\max}}$ indicate the primitive operator index that generated the maximum residue shown in $\mathcal{R}_\theta(f)$.

In the remainder of this section, we present some theoretical contributions of this paper, including properties of ultimate levelings and an efficient algorithm for ultimate leveling computation.

3.2. Properties of ultimate levelings

In this section, we will present two properties of ultimate levelings: structures preservation (in Section 3.2.1) and complementation (in Section 3.2.2). But, before that, it is worth mentioning that ultimate levelings are not morphological filters, i.e., they are not increasing and are also not idempotent, in spite of the ith residue r_i^+ (resp., r_i^-) is an idempotent operator, that is,

$$\begin{aligned} r_i^+(r_i^+(f)) &= \psi_i(r_i^+(f)) - \psi_{i+1}(r_i^+(f)) \vee 0 \\ &= \psi_i([\psi_i(f) - \psi_{i+1}(f) \vee 0]) - \psi_{i+1}([\psi_i(f) \\ &\quad -\psi_{i+1}(f) \vee 0]) \vee 0 \\ &= \psi_i([\psi_i(f) - \psi_{i+1}(f) \vee 0]) - 0 \\ &= \psi_i(f) - \psi_{i+1}(f) \vee 0 \\ &= r_i^+(f). \end{aligned}$$

We show as a contribution of this paper that ultimate levelings have very interesting properties on structures preservation (contours and regional extrema) and complementariness (see Sections 3.2.1 and 3.2.2, respectively). Moreover, positive ultimate levelings $\mathcal{R}_\theta^+$ are anti-extensive, i.e. $\mathcal{R}_\theta^+(f) \leq f$. Furthermore, a residual decomposition $(r_0(f), \ldots, r_{I_{MAX}-1}(f))$ of an image $f \in \mathcal{F}(\mathcal{D})$ can also be used to build residual hierarchies, and also it can be used for image reconstruction, since $r_i^+(f) = \psi_i(f) - \psi_{i+1}(f) \vee 0$ and $r_i^-(f) = \psi_{i+1}(f) - \psi_i(f) \vee 0$, we have that $\psi_i(f) = \psi_{i+1}(f) + r_i^+(f) - r_i^-(f)$, and, consequently, we can recon-

Fig. 7. Example of the associated image $q_{\mathcal{I}_{\max}}$ and the ultimate leveling $\mathcal{R}_\theta(f)$ of the input image presented in Fig. 6.

struct an image f from a residual decomposition as follows:

$$f = \psi_{I_{MAX}}(f) + \sum_{i=0}^{I_{MAX}-1} r_i^+(f) - \sum_{i=0}^{I_{MAX}-1} r_i^-(f). \tag{8}$$

3.2.1. Properties on structures preservation

Levelings are operators that satisfy good properties on structures preservation (contours and regional extrema). Indeed, these properties are widely desired in segmentation applications. In this section, we show that ultimate levelings inherit some of these properties.

Given an image f and a family of primitives $\{\psi_i : i \in \mathcal{I}\}$ indexed by a set $\mathcal{I}$, if $\psi_{i+1}(f)$ is a leveling of $\psi_i(f)$ and $(p,q) \in \mathcal{A}$, then $[\psi_i(f)](p) = [\psi_i(f)](q) \Rightarrow [\psi_{i+1}(f)](p) = [\psi_{i+1}(f)](q)$, which implies $[0 \vee \psi_i(f) - \psi_{i+1}(f)](p) = [0 \vee \psi_i(f) - \psi_{i+1}(f)](q)$ (resp. $[0 \vee \psi_{i+1}(f) - \psi_i(f)](p) = [0 \vee \psi_{i+1}(f) - \psi_i(f)](q)$), which shows that $r_i^+(f)$ (resp. $r_i^-(f)$) is connected of $\psi_i(f)$.

Besides, if $[\psi_{i+1}(f)](p) > [\psi_{i+1}(f)](q)$, then $[\psi_i(f)](p) \geq [\psi_{i+1}(f)](p) > [\psi_{i+1}(f)](q) \geq [\psi_i(f)](q)$, since $\psi_{i+1}(f)$ is a leveling of $\psi_i(f)$. Thus, we derive 2 statements: (*i*) $[0 \vee \psi_i(f) - \psi_{i+1}(f)](p) \geq [0 \vee \psi_i(f) - \psi_{i+1}(f)](q)$ (i.e., $[r_i^+(f)](p) \geq [r_i^+(f)](q)$); and (*ii*) $[\psi_i(f)](p) > [\psi_i(f)](q)$. Therefore, if $[\psi_{i+1}(f)](p) > [\psi_{i+1}(f)](q)$, then a transition on positive residues $r_i^+(f)$ implies a transition on $\psi_i(f)$ with the same order. We can come to the same conclusion, if we consider $[\psi_{i+1}(f)](p) = [\psi_{i+1}(f)](q)$. Therefore, $\forall (p,q) \in \mathcal{A}, [r_i^+(f)](p) \geq [r_i^+(f)](q) \Rightarrow [\psi_i(f)](p) > [\psi_i(f)](q)$, which shows also that $r_i^+(f)$ (resp., $r_i^-(f)$) is an arcwise connected operator (or monotone planing (Meyer, 1998a)) of $\psi_i(f)$. This leads us to Lemma 3.2.

Lemma 3.2. *If $(\psi_0(f), \psi_1(f), \ldots, \psi_n(f))$ is a scale-space based on levelings, then $r_i^+(f) = [0 \vee \psi_i(f) - \psi_{i+1}(f)]$ (resp., $r_i^-(f)$) is an arcwise connected operator of $\psi_i(f)$, for $0 \leq i \leq n-1$.*

On one hand, although connected operators never introduce new contours (Bangham et al., 1996b), they may turn a regional minimum into a maximum and vice-versa. On other hand, arcwise connected operators are a specialization of connected operators which do not create regional minima or maxima (Meyer, 1998a). Since levelings are a particular kind of arcwise connected operators, they share the same property. Besides, levelings also preserve order and this characteristic allows us to state Propositions 3.3 and 3.4. These propositions guarantee that ultimate levelings are also connected operators and preserve order. Note that, we can easily prove Propositions 3.3 and 3.4 with the help of Lemma 3.2 and the fact that connected (resp., arcwise connected and levelings) operators are closed under composition, infimum and supremum.

Proposition 3.3. *Ultimate levelings are connected operators.*

Proposition 3.4. *Positive (resp., negative) ultimate levelings are arcwise connected operators.*

Consequently, Propositions 3.3 and 3.4 lead us to Corollaries 3.5 and 3.6.

Corollary 3.5. *Ultimate grain filters are connected operators.*

Corollary 3.6. *Ultimate attribute openings (resp., closings) are arcwise connected operators.*

As positive (resp., negative) ultimate levelings are arcwise connected operators, and, therefore they will inherit the property of not creating regional maxima (resp., minima).

Proposition 3.7. *Positive ultimate levelings do not create new regional maxima. In other words, if $\mathcal{R}_\theta^+(f)$ (resp., $\mathcal{R}_\theta^-(f)$) has a regional maximum $\mathcal{X} \subseteq \mathcal{D}$, then f possesses a regional maximum (resp., minimum) $\mathcal{Z} \subseteq \mathcal{X}$.*

Proof. Let $\mathcal{X} \subseteq \mathcal{D}$ be a regional maximum of $\mathcal{R}_\theta^+(f)$ and let $y = \arg\max\{f(x) : x \in \mathcal{X}\}$ be a pixel of $\mathcal{X}$ with maximum value in f. Then, there is a flat-zone $\mathcal{Z}$ in f that contains y. Clearly, $\mathcal{Z} \subseteq \mathcal{X}$, since $\mathcal{R}_\theta^+$ is a connected operator. Now, suppose, by contradiction, that $\mathcal{Z}$ is not a regional maximum of f. Then, there is a pixel $p \notin \mathcal{Z}$ adjacent to some pixel $q \in \mathcal{Z}$ such that $f(p) > f(q) = f(y)$. Thanks to Proposition 3.4, we have that $\mathcal{R}_\theta^+$ is an arcwise connected operator. Thus, $f(p) \geq f(q) \Rightarrow [\mathcal{R}_\theta^+(f)](p) \geq [\mathcal{R}_\theta^+(f)](q)$, but as $q \in \mathcal{Z} \subseteq \mathcal{X}$ and $\mathcal{X}$ is a regional maximum of $\mathcal{R}_\theta^+(f)$, then $[\mathcal{R}_\theta^+(f)](p) = [\mathcal{R}_\theta^+(f)](q)$. So, $p \in \mathcal{X}$. However, this is a contradiction, since y is the pixel of $\mathcal{X}$ with maximum value in f, and, consequently, $f(p) \leq f(y)$. Therefore $\mathcal{Z}$ is a regional maximum of f. □

3.2.2. Properties with respect to complementation

Two operators ψ and φ are *dual* with respect to complementation if applying ψ to an image f is equivalent to applying φ to the complement of f and taking the complement of the result (Soille, 2005), i.e., $\psi(f) = [\varphi(f^c)]^c$, where f^c is the complement of image f and is defined, for each pixel $p \in \mathcal{D}$, as $f^c(p) = K - f(p)$. Similarly, ψ and φ are *complementary* if applying ψ to an image f is equivalent to applying φ to the *complement* of f, i.e. $\psi(f) = \varphi(f^c)$.

Proposition 3.8. *Let $(\psi_0(f), \psi_1(f), \ldots, \psi_n(f))$ and $(\varphi_0(f), \varphi_1(f), \ldots, \varphi_n(f))$ be two scale-spaces based on levelings such that for any $0 \leq i \leq n$, $\psi_i(f)$ is dual of $\varphi_i(f)$. Then, $r_i^+(f)$ and $r_i^-(f)$ are complementary, where $r_i^+(f) = [0 \vee \psi_i(f) - \psi_{i+1}(f)]$ and $r_i^-(f) = [0 \vee \varphi_{i+1}(f^c) - \varphi_i(f^c)]$.*

Proof.

$$\begin{aligned} r_i^+(f) &= [0 \vee \psi_i(f) - \psi_{i+1}(f)] \\ &= [0 \vee (\varphi_i(f^c))^c - (\varphi_{i+1}(f^c))^c] \\ &= [0 \vee (K - \varphi_i(f^c)) - (K - \varphi_{i+1}(f^c))] \\ &= [0 \vee \varphi_{i+1}(f^c) - \varphi_i(f^c)] \\ &= r_i^-(f^c) \end{aligned}$$

□

Corollary 3.9. *Ultimate attribute openings and closings are complementary.*

An operator ψ is *self-dual* with respect to complementation if its dual operator with respect to the complementation is ψ itself (Soille, 2005), i.e. $\psi(f) = [\psi(f^c)]^c$. Similarly, ψ is *self-complementary* if $\psi(f) = \psi(f^c)$.

Proposition 3.10. *Let $(\psi_0(f), \psi_1(f), \ldots, \psi_n(f))$ be a scale-space based on levelings such that $\psi_i(f)$ is self-dual. Then, we have that $r_i(f) = r_i^+(f) \vee r_i^-(f)$ is self-complementary.*

Corollary 3.11. *Ultimate grain filters are self-complementary.*

Corollary 3.12. *If $\mathcal{R}_\theta^+(f)$ is an ultimate attribute opening of f and $\mathcal{R}_\theta^-(f)$ is an ultimate attribute closing of f, then $[\mathcal{R}_\theta^+(f) \vee \mathcal{R}_\theta^-(f)]$ is self-complementary.*

3.3. Construction of ultimate levelings

Thanks to Theorem 2.7, it is known that if $(\mathcal{T}_f^0, \mathcal{T}_f^1, \ldots, \mathcal{T}_f^{I_{MAX}})$ is a sequence of trees obtained by successive prunings such that $\psi_0(f) = Rec(\mathcal{T}_f^0)$, $\psi_i(f) = Rec(\mathcal{T}_f^i)$ and $\mathcal{T}_f^i = \mathcal{P}runing(\mathcal{T}_f^{i-1})$, for $i \in \mathcal{I}$, then $(\psi_0(f), \psi_1(f), \ldots, \psi_{I_{MAX}}(f))$ constitutes a morphological scale-space based on levelings. Then, let $\mathcal{N}r(i)$ be the set of nodes removed from $\mathcal{T}_f^i$ to build the pruned tree $\mathcal{T}_f^{i+1}$, i.e. $\mathcal{N}r(i) = \mathcal{T}_f^i \setminus \mathcal{T}_f^{i+1}$. Since these trees are derived from successive prunings, we can present Proposition 3.13, which states that residues can be computed in parallel.

Proposition 3.13. *If $i, j \in \mathcal{I}$ such that $i \neq j$, then $\mathcal{N}r(i) \cap \mathcal{N}r(j) = \emptyset$.*

Therefore, we can calculate positive (resp., negative) residues of all pixels of a given node $C \in \mathcal{N}r(i)$ by

$$r^+_{\mathcal{T}_f^i}(C) = \begin{cases} [level(C) - level(\texttt{parent}(C)) \ \vee 0], & \text{if } \texttt{parent}(C) \notin \mathcal{N}r(i), \\ [level(C) - level(\texttt{parent}(C)) \ \vee 0] & \\ \quad + r^+_{\mathcal{T}_f^i}(\texttt{parent}(C)), & \text{otherwise,} \end{cases} \tag{9}$$

and thus,

$$\forall p \in \mathcal{D}, [r_i^+(f)](p) = \begin{cases} r^+_{\mathcal{T}_f^i}(\mathcal{SC}(\mathcal{T}_f^i, p)), & \text{if } \mathcal{SC}(\mathcal{T}_f^i, p) \in \mathcal{N}r(i), \\ 0, & \text{otherwise,} \end{cases} \tag{10}$$

and consequently, this leads us to Algorithm 1 for ultimate leveling computation through a top-down approach, which is a generalization of J. Fabrizio and B. Marcotegui's algorithm (Fabrizio and Marcotegui, 2009): (*i*) the residue of the parent node is calculated; (*ii*) it is then propagated to its child nodes; (*iii*) every child node compares its residue with the residue of its parent node and keeps the maximum of these two values in $\mathcal{R}_\theta$; (*iv*) after this step, each child node becomes a parent node and the process is repeated.

Algorithm 1: Basic computation of the ultimate levelings.

```
1  BasicComputationOfUltimateLeveling(Tree T_f, node C) begin
2      if ∃i ∈ I such that C ∈ Nr(i) then
3          r_i^+[C] = level(C) − level(parent(C)) ∨ 0;
4          r_i^−[C] = level(parent(C)) − level(C) ∨ 0;
5          if parent(C) ∈ Nr(i) then
6              r_i^+[C] = r_i^+[C] + r_i^+[parent(C)];
7              r_i^−[C] = r_i^−[C] + r_i^−[parent(C)];
8          R_θ^+[C] = R_θ^+[parent(C)] ∨ r_i^+[C];
9          R_θ^−[C] = R_θ^−[parent(C)] ∨ r_i^−[C];
           // From here, compute q^+ and q^−
10     foreach S ∈ children(C) do
11         BasicComputationOfUltimateLeveling (T_f, S);
```

The input of Algorithm 1 is a tree (max-tree, min-tree or tree of shapes). These trees can be built by simple algorithms based on union-find such as proposed in Berger et al. (2007); Géraud et al. (2013) with time complexity $O(|\mathcal{D}|\log(|\mathcal{D}|))$. Once the tree is built (see algorithms in Carlinet and Géraud (2013); Géraud et al. (2013)), function `BasicComputationOfUltimateLeveling`is executed from the root node. Conditions given at lines 2 and 5 depend on the chosen family of primitives and their verifications can be done in constant time. Since function `BasicComputationOfUltimateLeveling`visits each node of the tree exactly once and the number of nodes of the tree is at most the number of pixels in the image, `BasicComputationOfUltimateLeveling`is executed with time complexity $O(|\mathcal{D}|)$. At the end, we can reconstruct the output of Alg. 1 (i.e., $\forall p \in \mathcal{D}, \mathcal{R}_\theta(p) = \mathcal{R}_\theta^+[\mathcal{SC}(\mathcal{T}, p)] \vee \mathcal{R}_\theta^-[\mathcal{SC}(\mathcal{T}, p)]$) in $O(|\mathcal{D}|)$ time complexity. Therefore, the time complexity of the proposed algorithm is $O(|\mathcal{D}|\log(|\mathcal{D}|))$.

4. Strategies for choosing a family of primitives

The results of ultimate leveling operators depend directly on the chosen primitives. In fact, since residues are obtained by the difference of two consecutive primitives and they can be computed by the difference between two consecutive pruned trees, the output of Algorithm 1 depends on the set $\mathcal{N}r(i) = \mathcal{T}_f^i \setminus \mathcal{T}_f^{i+1}$ (see lines 2 and 5). Thus, a family of primitives $(\psi_0(f), \psi_1(f), \ldots, \psi_{I_{MAX}}(f))$ can be obtained by the reconstruction from a sequence of consecutive pruned trees $(\mathcal{T}_f^0 = \mathcal{T}_f, \mathcal{T}_f^1, \ldots, \mathcal{T}_f^{I_{MAX}})$, which in turn can be derived from the sets $\mathcal{N}r(i)$ by using the following formula:

$$\mathcal{T}_f^{i+1} = \mathcal{T}_f^i \setminus \mathcal{N}r(i). \tag{11}$$

The choice of $\mathcal{N}r(i)$ sets determines the pruning strategy. A logical predicate $\Gamma : \mathcal{P}(\mathcal{D}) \to \{\text{True}, \text{False}\}$ marks the tree branches to be pruned (see Algorithm 2). These markings (and consequently, every tree $\mathcal{T}_f^i$ and its set $\mathcal{N}r(i)$) can be obtained, for example, through a postorder traversal of $\mathcal{T}_f$. The node visiting order does not alter the ultimate leveling result thanks to Proposition 3.13. As an illustration, Fig. 6 shows an example of marking the tree (by sorting the height of CCs) in which we can deduce the sequence of nodes $\mathcal{N}r(i)$ and, consequently, the sequence of pruned trees.

Algorithm 2: Basic computation of choose a primitives family.

```
1  chooseThePrimitivesFamily tree T_f begin
2      i = 0
3      T_f^0 = T_f
4      foreach node C of a postorder traversal of T_f do
5          if Γ(C) is true then
6              Nr(i) is the subtree of T_f^i rooted in C
7              T_f^{i+1} = T_f^i \ Nr(i)
8              i = i + 1
```

Observe that the set with the largest number of primitives that can be derived from a tree $\mathcal{T}_f$ is given by the criterion: $\forall C \in \mathcal{T}_f$, $\Gamma(C) = [\![C \text{ is not root}]\!]$. It can be a good idea to use all these primitives if the purpose involves shape recognition. However, that does not seem to be a good idea if the purpose is to identify contrasted regions from a natural image, since the residue generated between two consecutive operators can be very close to zero. This may occur because the objects of an image decompose very slowly. Thus, in the following subsections, we present some strategies to build

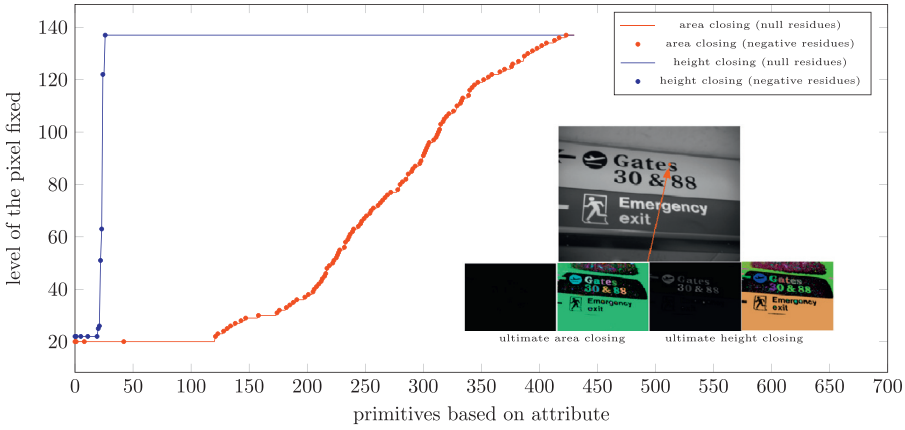

Fig. 8. Evolution of residual values of the pixel marked in red of the input image obtained from ultimate attribute (area and height) closings. (For interpretation of the references to color in this figure legend, the reader is referred to the web version of this article.)

primitive families that can generate more significant residues for the ultimate levelings.

4.1. Attribute based primitives

As stated in Section 2, tree nodes correspond to image regions defined by level sets. Characteristics of these regions such as area, volume, height, width or circularity can be computed and assigned to tree nodes as node attributes. Several attributes can be combined in a vector, as proposed in Urbach et al. (2005), but in this paper only scalar attributes are considered. Thus, formally, a node attribute is a function $\kappa : \mathcal{P}(\mathcal{D}) \to \mathbb{R}$ representing a region feature. Some attributes are increasing, i.e., $A, B \in \mathcal{P}(\mathcal{D}), A \subseteq B \Rightarrow \kappa(A) \leq \kappa(B)$. If attributes are increasing, their values also follow a well-defined ordering in the tree due to the hierarchy of the level sets. Thanks to this property, attribute opening (resp., closing and grain filter) is performed by simply pruning the tree nodes whose attribute value κ is lower than a given threshold t followed by reconstruction of the pruned tree. For non increasing attributes several strategies (min, max, direct or Viterbi optimization) are proposed in Salembier et al. (1998).

Thus, families of attribute openings, attribute closings and grain filters can be determined from a family of increasing thresholds $(t_1, t_2, \ldots, t_{I_{MAX}})$ for an increasing attribute κ. For example, the family of thresholds can be derived from a tree $\mathcal{T}_f$, i.e., $t_i \in T_\kappa = \{\kappa(C) : C \in \mathcal{T}_f\}$ such that $1 \leq i \leq |T_\kappa| = I_{MAX}$. Thus, $\mathcal{T}_f^0 = \mathcal{T}_f$, $\mathcal{T}_f^{i+1} = Pruning(\mathcal{T}_f^i) = \{C \in \mathcal{T}_f^i : \kappa(C) \leq t_{i+1}\}$ and $\psi_i = Rec(\mathcal{T}_f^i)$, for $0 \leq i < I_{MAX}$. Therefore, a node $C \in \mathcal{N}r(i) = \mathcal{T}_f^i \setminus \mathcal{T}_f^{i+1}$ satisfies the conditions of criterion Γ, if and only if, $\kappa(C) \leq t_i$ and $\kappa(\texttt{parent}(C)) > t_i$ or equivalently $\kappa(C) \neq \kappa(\texttt{parent}(C))$ So, $\forall N \in \mathcal{T}_f, \Gamma(N) = [\![\kappa(N) \neq \kappa(\texttt{parent}(N))]\!]$.

Residual values of negative (resp. positive) ultimate levelings $\mathcal{R}_\theta^-$ (resp. $\mathcal{R}_\theta^+$) are the biggest difference between two consecutive operators from a given primitive family. In this sense, Fig. 8 shows an example of an application of $\mathcal{R}_\theta^-$ in a given image $f \in \mathcal{F}(\mathcal{D})$ where we analyze the evolution of residual values for a given pixel using two primitive families: area closing and height closing.

Primitive families based on area attribute (or similarly, volume) tend to simplify images very slowly leading to very small residues. We can get bigger residues if we choose primitive families that tend to simplify the image more quickly, as evidenced in Fig. 8: family of height closings simplifies more quickly than family of area closings. In both cases, we see that the residues generated for the selected pixel are the largest transition between two consecutive primitives, which are the following: 2 for area closings and 59 for height closings, but, in both cases, they are smaller than the real contrast (that is, approximately 117) of the object that contains the selected pixel.

Based on these considerations, Marcotegui et al. (2011), proposed a solution for primitive selection called *gradual transition* and, in this paper, we propose a second solution, based on extinction values (Grimaud, 1992; Vachier and Meyer, 1995).

- *Primitives based on gradual transition*
  As seen previously, families of attribute openings (resp. closings) and grain filters can be determined from families of increasing thresholds $(t_1, \ldots, t_{I_{MAX}})$ for an increasing attribute κ. Thus, a node $C \in \mathcal{N}r(i) \subseteq \mathcal{T}_i$ satisfies the conditions of criterion Γ, if and only if, $\kappa(C) \leq t_i$ and $\kappa(\texttt{parent}(C)) > t_i$ or equivalently $\kappa(C) \neq \kappa(\texttt{parent}(C))$ which also is equivalent to $\kappa(\texttt{parent}(C)) - \kappa(C) > 0$. Thus, one way to reduce this discomfort is to mark the nodes that have a great variation Δ of attribute value with respect to its parent, i.e., $C \in \mathcal{T}_f$ satisfies the conditions of criterion Γ, if and only if, $\kappa(\texttt{parent}(C)) - \kappa(C) > \Delta$. So, $\forall N \in \mathcal{T}_f$, we do: $\Gamma(N) = [\![\kappa(\texttt{parent}(N)) - \kappa(N) > \Delta]\!]$.
  Note that, choosing $\Delta = 0$ gives the classic ultimate leveling, $\Delta = 1$ integrates a series of non-null residues, $\Delta = 2$ integrates a series of residues separated by at least 2 consecutive null residues, and so on (Marcotegui et al., 2011). Note that, it is not easy to find the best value for Δ, since it is a global information and is not always possible to estimate the real contrast for all regions of the image.
- *Primitives based on extinction values*
  Extinction values (Grimaud, 1992; Vachier and Meyer, 1995) are good candidates to define a pruning predicate Γ. Extinction values are measures extracted from regional extrema (minima or maxima). In short, the extinction value of a regional extremum M for an increasing attribute κ is the maximal size of the attribute filter, such that there still exists a regional extremum M' that contains M after the filtering (Grimaud, 1992; Vachier and Meyer, 1995). Thus, we can mark only the nodes such that their attribute value corresponds to an extinction value. This procedure can be done by the following algorithm (Silva and de Alencar Lotufo, 2011):
  1. For each leaf L of $\mathcal{T}_f$ (i.e. regional extremum), the path towards the root is initiated.
     (a) When a node N_L with more than one child appears (i.e. a ramification) in the path, the following verification is performed:
        i. Let $C_L \in \texttt{children}(N_L)$ be the node such that $L \subset C_L$ (i.e., C_L is ancestral of L). If there exists another $C \in \texttt{children}(N_L)$ such that $\kappa(C) > \kappa(C_L)$, then $\kappa(C_L)$ is defined as the extinction value for leaf L (note that,

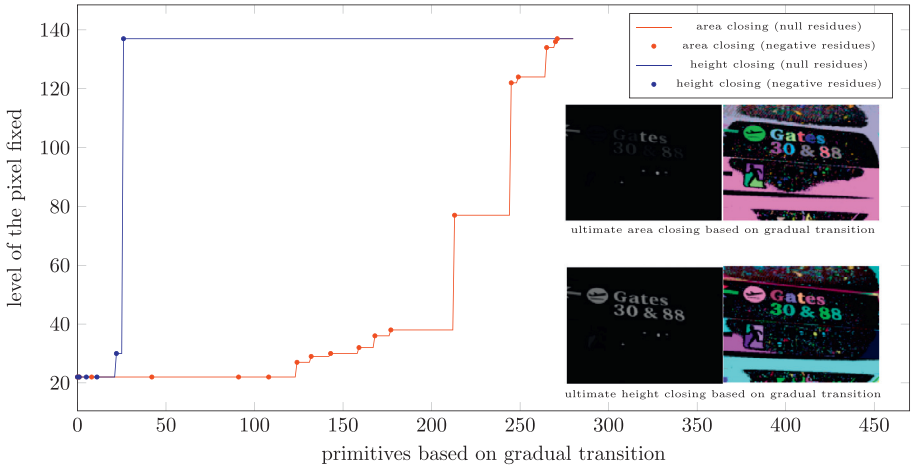

Fig. 9. Evolution of residual values of the pixel marked in red of the input image obtained from ultimate attribute (area and height) closings using a family of primitives based on gradual transition. (see Fig. 8). (For interpretation of the references to color in this figure legend, the reader is referred to the web version of this article.)

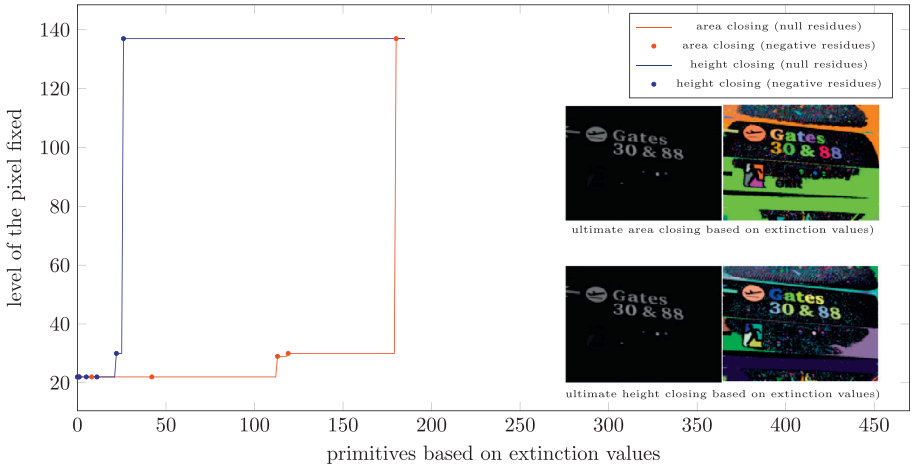

Fig. 10. Evolution of residual values of the pixel marked in red of the input image obtained from ultimate attribute (area and height) closings using a family of primitives based on extinction values. (For interpretation of the references to color in this figure legend, the reader is referred to the web version of this article.)

in this case, this is the maximum attribute value that maintains the regional extremum L (Silva and de Alencar Lotufo, 2011)). Thus, $\Gamma(C)$ is true for all $C \in \texttt{children}(N_L)$ and then an iteration for the next leaf is performed.

ii. Otherwise, we continue the leaf path until the next ramification N_L is found and the procedure is repeated.

iii. Finally, if the path reaches the root, then its extinction value is set as the attribute value of the first node in the path before arriving at the root, which is the maximum image extinction value.

Fig. 10 shows the evolutions of residual values of a given pixel obtained from ultimate attribute closings based on extinction values. As we can see, comparing with the ones of Fig. 9, the residual values using height attribute with extinction value strategy are bigger than the ones obtained by using gradual transitions.

A summary of this section is illustrated on Fig. 11. Applications of ultimate levelings based on different families of primitives are shown highlighting the following aspects: (*i*) polarity of objects extracted from ultimate levelings: light (resp. dark) objects are residues extracted from anti-extensive (resp. extensive) primitives as attribute openings (resp. attribute closings) and objects in both polarities are residues extracted from self-dual primitives as grain filters; (*ii*) the choice of attribute type: attribute filters that simplify images more slowly, such as area attribute ones, tend to produce less contrast, whereas attribute filters that simplify images more abruptly tend to produce more contrast such as height attribute filters. (*iii*) the choice of a strategy for selecting primitives that produce more contrast such as primitives based on gradual transition or on extinction values. In this way, we should remark that the parameter Δ for selecting primitives based on gradual transition is a global information so that it is not always possible to estimate real contrast for all regions of the image, whereas extinction values are obtained from local information of the image associated to regional extrema and this makes them good alternatives to design non-parametric ultimate levelings.

4.2. Primitives based on marked image

Primitives based on marked image can be obtained by a traditional algorithm Λ, such as the one originally proposed by Meyer (1998b), to construct levelings that takes two images as arguments: an input image $f \in \mathcal{F}(\mathcal{D})$ and a marker image $g \in \mathcal{F}(\mathcal{D})$. It modifies g in such a way that it becomes a leveling of f. Let us denote by $\Lambda(f, g)$ the leveling of f obtained from marker g.

It can be shown that anti-extensive (resp. extensive) levelings, named opening by reconstruction (resp. closing by reconstruction), can be constructed from marker images. They can be ob-

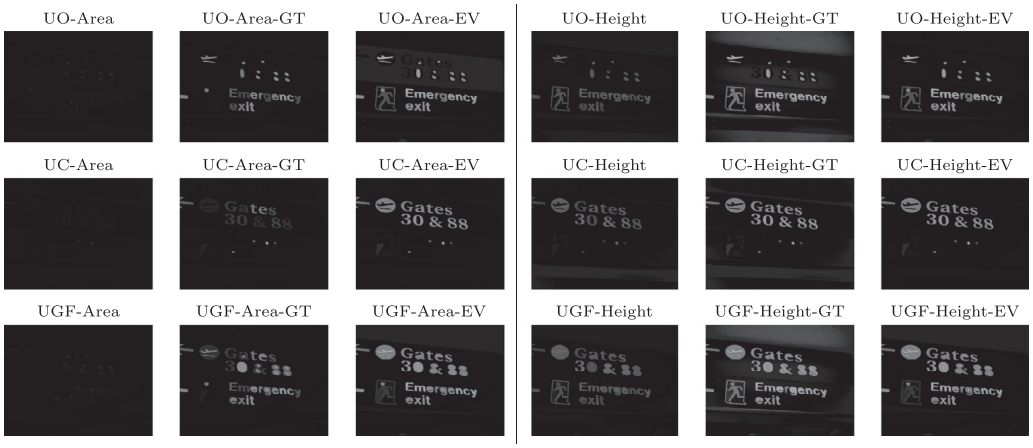

Fig. 11. Example of applications of ultimate levelings where each row contains applications of UAO, UAC and UGF using primitive families based on attributes (area and height of bounding box), gradual transition (GT) with $\Delta = 5$ and extinction values (EV).

tained by pruning operations of extended max-trees (resp. min-trees) (Alves et al., 2015). In this case, the nodes of the tree to be pruned are determined according to the image marker (Alves et al., 2015). Then, let $\mathcal{T}_\rho(\mathcal{T}_f, g)$ and $\mathcal{T}_{\rho^*}(\mathcal{T}_f, g)$ denote the trees obtained from, respectively, an opening and a closing by reconstruction of tree $\mathcal{T}_f$ by marked image $g \in \mathcal{F}(\mathcal{D})$. Thus, families of openings (resp. closings) by reconstruction $(\psi_0(f), \psi_1(f), \ldots, \psi_{I_{MAX}}(f))$ can be determined from families of markers $(g_1, g_2, \ldots, g_{I_{MAX}})$ in the following way: $\mathcal{T}_0 = \mathcal{T}_f$, $\psi_0(f) = Rec(\mathcal{T}_0) = f$, $\mathcal{T}_i = Pruning(\mathcal{T}_{i-1}) = \mathcal{T}_\rho(\mathcal{T}_{i-1}, g_i)$ (resp. $\mathcal{T}_{\rho^*}(\mathcal{T}_{i-1}, g_i)$) and $\psi_i(f) = Rec(\mathcal{T}_i)$ for $1 \leq i < I_{MAX}$. Thus, families of markers may be used to generate morphological scale-spaces based on levelings as shown by Meyer and Maragos (2000) and Meyer (2010).

If primitives are neither extensive nor anti-extensive, then we can separately calculate positive and negative ultimate levelings and after combine them (see Proposition 16 in Meyer (1998a)).

In general, $\mathcal{N}r(i)$ is a set of connected components of graph $\mathcal{T}_i \setminus \mathcal{T}_{i+1}$ and, consequently, a node $C \in \mathcal{N}r(i) \subseteq \mathcal{T}_i$ satisfies the conditions of criterion Γ, if and only if node C is removed (and, at the same time, its parent node is preserved) by the pruning operation generated by the corresponding marker image.

5. Strategies for filtering undesirable residues

Ultimate levelings are operators that extract residual information from primitive families. During the residual extraction process, it is very common that undesirable regions of the input image contain residual information that should be filtered out. These undesirable residual regions often include desirable residual regions (which should be preserved) due to the design of the ultimate levelings which consider maximum residues.

Retornaz (2007) already described this problem, called myopia, which is normally produced by nested structures (in fact, this can be confirmed by Proposition 3.7). In this way, Hernández and Marcotegui (2011) proposed a solution for this problem using shape information during the residual extraction process. However, the drawback of this solution is that residual values are modified according to a similarity function and thus the properties of ultimate levelings are lost.

In this work, we propose an approach to preserve the original extracted residual values while filtering out residues extracted from undesirable regions. As shown in Fig. 12, we calculate ultimate levelings $\mathcal{R}_\theta$ only for residues r_i satisfying a given similarity criterion Ω.

This procedure can be implemented in several manners. To decide whether a residue $r_i^+(f)$ (resp., $r_i^-(f)$) is filtered out or not,

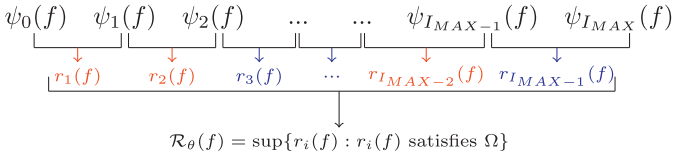

Fig. 12. Scheme for filtering out residues r_i extracted from undesirable regions. For example, the residues in red do not satisfies the criterion Ω and thereby they are filtered out; the supremum is evaluate only on the blue ones. (For interpretation of the references to color in this figure legend, the reader is referred to the web version of this article.)

just checking nodes $C \in \mathcal{N}r(i)$ that satisfy a given filtering criterion $\Omega : \mathcal{P}(\mathcal{D}) \to \{\text{desirable}, \text{undesirable}\}$. Thus, we only calculate the ultimate leveling $\mathcal{R}_\theta$ for residues r_i^+ (resp., r_i^-) such that satisfy the criterion Ω. So, positive (resp. negative) residues are redefined as follows:

$$\forall p \in \mathcal{D}, [r_i^{\Omega+}(f)](p) = \begin{cases} r^+_{\mathcal{T}_f^i}(\mathcal{SC}(\mathcal{T}_f^i, p)), & \text{if } \mathcal{SC}(\mathcal{T}_f^i, p) \in \mathcal{N}r(i) \text{ and } \exists C \in \mathcal{N}r(i) \\ & \text{such that } \Omega(C) \text{ is desirable;} \\ 0, & \text{otherwise.} \end{cases} \tag{12}$$

Ultimate levelings obtained from filtering out undesirable regions are redefined as follows:

$$\mathcal{R}_\Omega(f) = \mathcal{R}^+_\Omega(f) \vee \mathcal{R}^-_\Omega(f), \tag{13}$$

where,

$$\mathcal{R}^+_\Omega(f) = \sup\{r_i^{\Omega+}(f) : i \in \mathcal{I}\} \text{ and } \mathcal{R}^-_\Omega(f) = \sup\{r_i^{\Omega-}(f) : i \in \mathcal{I}\}. \tag{14}$$

Below are listed two examples for filtering strategy. The first one is based on feature vector (Urbach et al., 2005; 2007) similar to the research from Hernández and Marcotegui (2011) and the second one is based on stable regions (Matas et al., 2004).

5.1. Filtering based on shape information

Shape recognition is one of the fundamental problems in field of image analysis and various approaches have been proposed over the last decades. One of the shape recognition subproblems is called decision problem (Hernández and Marcotegui, 2011; Veltkamp and Hagedoorn, 2000) that consists in comparing two patterns A and B using a similarity measure $d : \mathcal{P}(\mathcal{D}) \times \mathcal{P}(\mathcal{D}) \to \mathbb{R}_+$

Please cite this article as: W.A.L. Alves et al., Ultimate levelings, Computer Vision and Image Understanding (2017), http://dx.doi.org/10.1016/j.cviu.2017.06.010

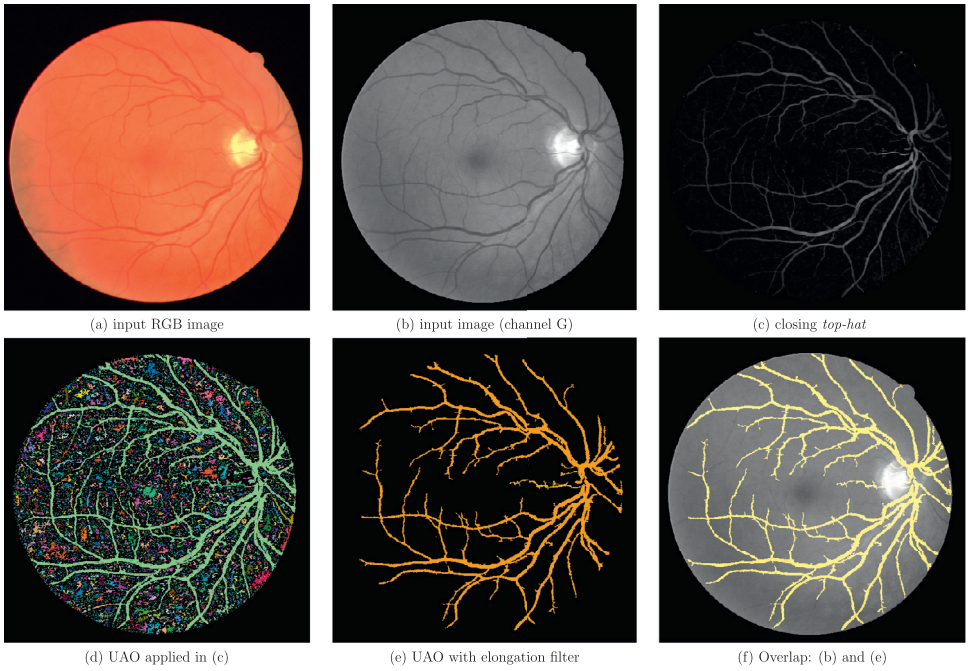

(a) input RGB image (b) input image (channel G) (c) closing *top-hat*

(d) UAO applied in (c) (e) UAO with elongation filter (f) Overlap: (b) and (e)

Fig. 13. Application of ultimate leveling (ultimate attribute opening) with elongation shape information.

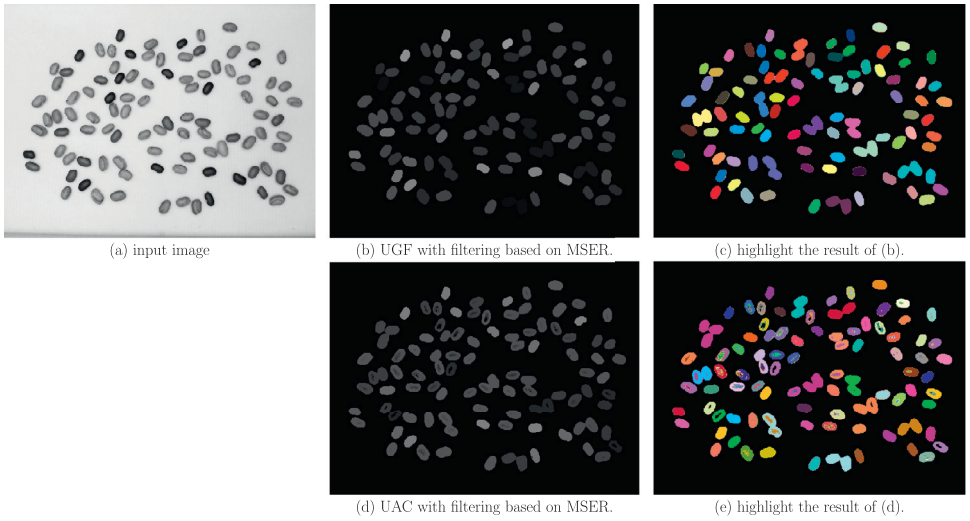

(a) input image (b) UGF with filtering based on MSER. (c) highlight the result of (b).

(d) UAC with filtering based on MSER. (e) highlight the result of (d).

Fig. 14. Example of applications of ultimate levelings for beans segmentation.

by means of a given threshold α, that is, deciding whether the similarity is greater or smaller than the threshold. Thus, we can construct Ω according to a similarity criterion, comparing the shape corresponding to a node $C \in \mathcal{N}r(i)$ and a reference shape $\Omega_{ref} \in \mathcal{P}(\mathcal{D})$. Thus, the criterion Ω is defined for any node $C \in \mathcal{P}(\mathcal{D})$ as follows:

$$\Omega(C) = \begin{cases} \text{desirable}, & \text{if } d(C, \Omega_{ref}) \leq \alpha, \\ \text{undesirable}, & \text{otherwise.} \end{cases} \tag{15}$$

This filtering strategy was first introduced by Hernández and Marcotegui (2011) where several shape similarity functions were studied.

5.2. Filtering based on maximally stable extremal regions

Maximally Stable Extremal Regions (MSER) originally introduced by Matas et al. (2004) have been widely used in a variety of applications in computer vision as region detector. The regions detected by this method are the CCs of level sets with maximum stability and, as shown by Kimmel et al. (2011), are invariant to affine transformations and thereby this method has an advantage compared to the SIFT detector. In this way, stability can be seen as a relationship between intensities and attributes of comparable CCs. More formally, a *stability function* associates to any CC C_λ, extracted from a level set at value λ, the following value:

$$Stability(C_\lambda) = \frac{\kappa(C_\lambda)}{|\kappa(C_{\lambda-\Delta}) - \kappa(C_{\lambda+\Delta})|}, \tag{16}$$

where $\Delta \in \mathbb{K}$ is a stability parameter and $C_{\lambda-\Delta}$, C_λ and $C_{\lambda+\Delta}$ are comparable CCs extracted from level sets at values, $\lambda - \Delta$, λ and $\lambda + \Delta$, respectively. Then, the CCs that correspond to the local maxima of stability function are called MSERs. It is worth mentioning that MSER variants (Kimmel et al., 2011; Xu et al., 2014) can be explored.

Please cite this article as: W.A.L. Alves et al., Ultimate levelings, Computer Vision and Image Understanding (2017), http://dx.doi.org/10.1016/j.cviu.2017.06.010

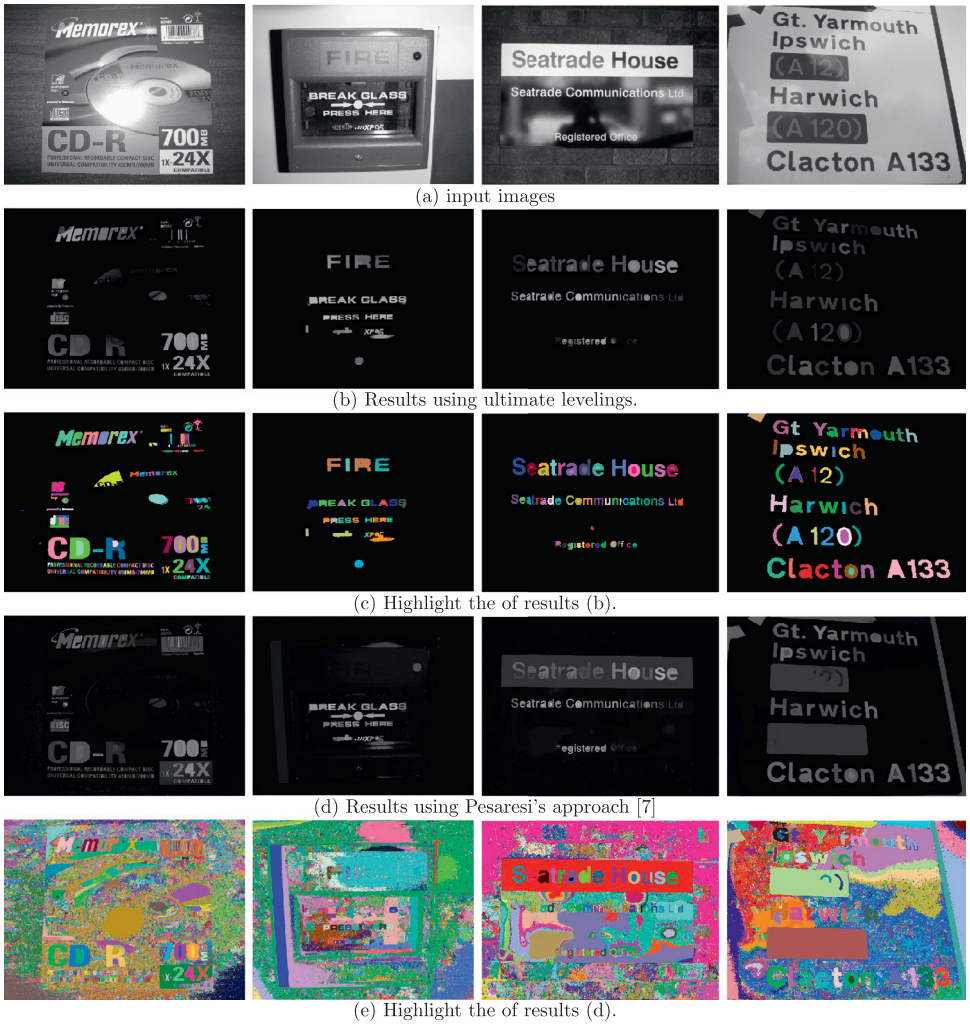

(a) input images

(b) Results using ultimate levelings.

(c) Highlight the of results (b).

(d) Results using Pesaresi's approach [7]

(e) Highlight the of results (d).

Fig. 15. Application of ultimate grain filter with composite filter.

Based on these considerations, the criterion Ω is defined for any node $C \in \mathcal{P}(\mathcal{D})$ as follows:

$$\Omega(C) = \begin{cases} \text{desirable}, & \text{if } C \text{ is MSER}, \\ \text{undesirable}, & \text{otherwise.} \end{cases} \tag{17}$$

6. Examples of application of ultimate levelings

This section provides some illustrative examples of application of ultimate levelings in order to give a glimpse of their usefulness.

6.1. Blood vessels segmentation

Blood vessels segmentation from images such as of Fig. 13a is a very important problem for retinal image analysis. Since ultimate levelings preserve location and shape of contours, it is appropriate to apply them along with a shape-based filter such as presented in Section 5.1. In fact, an approach is to first apply the closing top-hat operator (with a disk-shaped structuring element with a radius of 7 pixels) in order to reduce the amount of undesirable information (see Fig. 13c); and, then, apply an ultimate leveling with anti-extensive primitives and using a filter that emphasizes elongated objects defined as (although other definitions can be found at Lantuejoul and Beucher (1981); Morard et al. (2013); Serna et al. (2014)):

$$\Omega_{\text{elongation}}(C) = \begin{cases} \text{desirable}, & \text{if } d(C, \Omega_{ref}) = \dfrac{1}{E(C)} \leq \alpha, \\ \text{undesirable}, & \text{otherwise.} \end{cases} \tag{18}$$

where $E(C) = \pi\ \text{SemiMajorAxis}(C)^2/(4\ \text{Area}(C))$ is the elongation measure (Xu et al., 2013), obtained from Area(C) and SemiMajorAxis(C) which are, respectively, the area of CC (or shape) C and the length of semi-major axis of the best fitting ellipse on C computed by central moments.

We can see in Fig. 13e the result of this application. Just for comparison, Fig. 13d shows an application of ultimate levelings without applying elongation filtering. As we can observe, the elongation filter significantly improves the result.

6.2. Beans segmentation

Automated systems for inspection of agricultural products are very relevant for classification, quality estimation, and storage supervision of fruits and vegetables. In particular, since bean constitutes the staple diet of people in some countries, their visual quality inspection could reduce significantly the time-consuming and high-cost of manual inspection task. One step to accomplish this automated inspection is to obtain a segmentation of beans

Please cite this article as: W.A.L. Alves et al., Ultimate levelings, Computer Vision and Image Understanding (2017), http://dx.doi.org/10.1016/j.cviu.2017.06.010

from images such as of Fig. 14a. For that, we can apply ultimate levelings using grain filters (Fig. 14b and c) or attribute closings (Fig. 14d and e) as primitives along with filtering based on MSER, as discussed in Section 5.2. As we can see, the ultimate levelings using grain filters as primitives were able to segment the whole bean with no holes, since grain filters are self-dual operators.

6.3. Scene-text detection

Texts present within scenes are usually associated to digital media semantic contexts and may constitute important content-based descriptors. In particular, the problem of separating text from non-text regions in images, such as the ones presented in Fig. 15 taken from ICDAR dataset (Lucas et al., 2003), is a step to solve the scene-text detection problem. One approach is to solve another supervised classification problem that comes first which consists of deciding whether a connected component is a character or not. For that, we can define some features (descriptors) used in scene-text detection problems (Alves and Hashimoto, 2010; Alves et al., 2013; Retornaz and Marcotegui, 2007) such as: aspect ratio (H_1), rectangularity (H_2), number of holes (H_3) and color variance (H_4). From them, given a set of thresholds $\alpha_i, \beta_i \in \mathbb{R}_+$, for $i = 1, 2, 3, 4$, we can build logical predicates $\Gamma_i(C) = [\![\alpha_i \leq H_i(C) \leq \beta_i]\!]$. For the purpose of this application, we used:

$$\begin{aligned} &\Gamma_1(C) = 0 \leq H_1(C) \leq 8 \\ &\Gamma_2(C) = 0,4 \leq H_2(C) \leq 0.95 \\ &\Gamma_3(C) = 0 \leq H_3(C) \leq 5 \\ &\Gamma_4(C) = 0 \leq H_4(C) \leq 60 \end{aligned} \tag{19}$$

These logical predicates can be used along with filtering based on MSER in the following way:

$$\Omega_{\text{char}}(C) = \begin{cases} \text{desirable}, & \text{if } C \text{ is MSER and } \Gamma_i(C) \text{ are all true,} \\ & \text{for } i = 1, \ldots, 4, \\ \text{undesirable}, & \text{otherwise.} \end{cases} \tag{20}$$

The ultimate leveling with this composite filter can be used in a first step of scene-text detection problems in which a set of candidate characters is extracted and then a set of candidate text regions is constructed by merging candidate characters. Thus, these candidate text regions are classified as text or non-text regions (Alves and Hashimoto, 2010; Fabrizio et al., 2013; Retornaz and Marcotegui, 2007). Fig. 15c shows the results of application of ultimate levelings in some images (presented at Fig. 15a) of ICDAR dataset (Lucas et al., 2003). It is worth mentioning that text regions are extracted even in images with both polarities, low contrast, complex background and illumination problems. Just for comparison, Fig. 15e shows the results of application of Pesaresi's approach (Pesaresi and Benediktsson, 2000). As we can observe, the ultimate levelings along with a composite MSER-based filter significantly improves the result generating images without noises.

7. Conclusion

This work presents a new class of residual operators called ultimate levelings which are powerful multi-scale image operators defined on levelings scale-space. Besides, other contributions of this paper include: (*i*) the statement of properties of ultimate levelings (in Section 3.2), (*ii*) the presentation of an efficient algorithm for their computation inspired by Fabrizio and Marcotegui's algorithm (Fabrizio and Marcotegui, 2009) (in Section 3.3), (*iii*) the provision of strategies for choosing families of primitives (in Section 4), (*iv*) the presentation of strategies for filtering undesirable residues (in Section 5), (*v*) the provision of some illustrative examples (retinal blood vessels extraction, beans segmentation and text location) of application of ultimate levelings (in Section 6).

Furthermore, ultimate levelings are computationally efficient and their performance evaluations are comparable to the state of art methods for filtering and image segmentation. For example, some operators included in ultimate levelings class have been demonstrated to have good perfomance evaluation (Alves and Hashimoto, 2010; 2014; Hernández and Marcotegui, 2011; Li et al., 1997; Retornaz and Marcotegui, 2007). We also provide a plugin and source code for the popular free image processing software ImageJ (Rasband, 1997) that gives access for some ultimate levelings operators. Instructions for download and installation can be found at http://www.ime.usp.br/~wonder/UL.

As a future work, in order to avoid nesting of residual regions, we plan to analyze a series of residues between nodes and, using a certain criterion, take a global decision for selecting the best residues.

Acknowledgments

This paper was financially supported by CAPES, CNPq and FAPESP (grant number: 2016/02547-5).

References

Alves, W., Hashimoto, R., 2010. Text regions extracted from scene images by ultimate attribute opening and decision tree classification. In: Proceedings of the 23rd SIBGRAPI Conference on Graphics, Patterns and Images, pp. 360–367.
Alves, W., Morimitsu, A., Castro, J., Hashimoto, R., 2013. Extraction of numerical residues in families of levelings. In: Graphics, Patterns and Images (SIBGRAPI), 2013 26th SIBGRAPI - Conference on, pp. 349–356.
Alves, W.A.L., Hashimoto, R.F., 2014. Ultimate grain filter. In: IEEE International Conference on Image Processing, pp. 2953–2957. Paris, France.
Alves, W.A.L., Morimitsu, A., Hashimoto, R.F., 2015. Scale-space representation based on levelings through hierarchies of level sets. In: Proceedings of the 12th International Symposium on Mathematical Morphology and its Applications to Image and Signal Processing. In: Lecture Notes in Computer Science, 9082, pp. 265–276.
Bangham, J.A., Chardaire, P., Pye, C.J., Ling, P.D., 1996a. Multiscale nonlinear decomposition: the sieve decomposition theorem. IEEE Trans. Pattern Anal. Mach. Intell. 18 (5), 529–539.
Bangham, J.A., Ling, P.D., Harvey, R., 1996b. Scale-space from nonlinear filters. IEEE Trans. Pattern Anal. Mach. Intell. 18, 520–528.
Berger, C., Géraud, T., Levillain, R., Widynski, N., Baillard, A., Bertin, E., 2007. Effective component tree computation with application to pattern recognition in astronomical imaging. In: IEEE International Conference on Image Processing, 4. IV–41–IV–44.
Beucher, S., 2007. Numerical residues. Image Vis. Comput. 25 (4), 405–415.
Carlinet, E., Géraud, T., 2013. A comparison of many max-tree computation algorithms. In: Mathematical Morphology and Its Applications to Signal and Image Processing, 7883. Springer Berlin Heidelberg, pp. 73–85.
Caselles, V., Meinhardt, E., Monasse, P., 2008. Constructing the tree of shapes of an image by fusion of the trees of connected components of upper and lower level sets. Positivity 12 (1), 55–73.
Caselles, V., Monasse, P., 2010. Geometric Description of Images as Topographic Maps. Springer-Verlag Berlin Heidelberg.
Dalla Mura, M., Benediktsson, J.A., Waske, B., Bruzzone, L., 2010. Morphological attribute profiles for the analysis of very high resolution images. IEEE Trans. Geosci. Remote Sens. 48 (10), 3747–3762.
Fabrizio, J., Marcotegui, B., 2009. Fast implementation of the ultimate opening. In: Proceedings of the 9th International Symposium on Mathematical Morphology, pp. 272–281.
Fabrizio, J., Marcotegui, B., Cord, M., 2013. Text detection in street level images. Pattern Anal. Appl. 16 (4), 519–533.
Géraud, T., Carlinet, E., Crozet, S., Najman, L., 2013. A quasi-linear algorithm to compute the tree of shapes of nd images. In: Mathematical Morphology and Its Applications to Signal and Image Processing. Lecture Notes in Computer Science. Springer Berlin Heidelberg, pp. 98–110.
Ghamisi, P., Dalla Mura, M., Benediktsson, J.A., 2015. A survey on spectral-spatial classification techniques based on attribute profiles. IEEE Trans. Geosci. Remote Sens. 53 (5), 2335–2353.
Grimaud, M., 1992. New measure of contrast: the dynamics. In: In SPIE Image Algebra and Morphological Image Processing III, 1769, pp. 292–305.
Hernández, J., Marcotegui, B., 2011. Shape ultimate attribute opening. Image Vis. Comput. 29 (8), 533–545.
Kimmel, R., Zhang, C., Bronstein, A., Bronstein, M., 2011. Are MSER features really interesting? Pattern Anal. Mach. Intell. IEEE Trans. 33 (11), 2316–2320.
Lantuejoul, C., Beucher, S., 1981. On the use of the geodesic metric in image analysis. J. Microsc. 121 (1), 39–49.

Li, W., Haese-Coat, V., Ronsin, J., 1997. Residues of morphological filtering by reconstruction for texture classification. Pattern Recognit. 30 (7), 1081–1093.
Lucas, S.M., Panaretos, A., Sosa, L., Tang, A., Wong, S., Young, R., 2003. ICDAR 2003 robust reading competitions. In: ICDAR03, 2, p. 682.
Marcotegui, B., Hernández, J., Retornaz, T., 2011. Ultimate opening and gradual transitions. In: Soille, P., Pesaresi, M., Ouzounis, G. (Eds.), Mathematical Morphology and Its Applications to Image and Signal Processing. Lecture Notes in Computer Science, 6671. Springer Berlin Heidelberg, pp. 166–177.
Matas, J., Chum, O., Urban, M., Pajdla, T., 2004. Robust wide-baseline stereo from maximally stable extremal regions. Image Vis. Comput. 22 (10), 761–767. British Machine Vision Computing 2002.
Meyer, F., 1998a. From connected operators to levelings. In: Proceedings of the 4th International Symposium on Mathematical Morphology and its Applications to Image and Signal Processing, pp. 191–198.
Meyer, F., 1998b. The levelings. In: Proceedings of the 4th International Symposium on Mathematical Morphology and its Applications to Image and Signal Processing, pp. 199–206.
Meyer, F., 2004. Levelings, image simplification filters for segmentation. J. Math. Imaging Vis. 20 (1–2), 59–72.
Meyer, F., 2010. Levelings and flat zone morphology. In: 2010 20th International Conference on Pattern Recognition, pp. 1570–1573.
Meyer, F., Maragos, P., 2000. Nonlinear scale-space representation with morphological levelings. J. Vis. Commun. Image Represent. 11 (2), 245–265.
Monasse, P., Guichard, F., 2000. Fast computation of a contrast-invariant image representation. IEEE Trans. Image Process. 9 (5), 860–872.
Morard, V., Decenciere, E., Dokládal, P., 2013. Efficient geodesic attribute thinnings based on the barycentric diameter. J. Math. Imaging Vis. 46 (1), 128–142.
Najman, L., Talbot, H., 2013. Mathematical Morphology. John Wiley & Sons.
Ouzounis, G.K., Pesaresi, M., Soille, P., 2012. Differential area profiles: decomposition properties and efficient computation. IEEE Trans. Pattern Anal. Mach. Intell. 34 (8), 1533–1548.
Pesaresi, M., Benediktsson, J., 2000. Image segmentation based on the derivative of the morphological profile. In: Goutsias, J., Vincent, L., Bloomberg, D. (Eds.), Mathematical Morphology and its Applications to Image and Signal Processing. Computational Imaging and Vision, 18. Springer US, pp. 179–188.
Pesaresi, M., Benediktsson, J., 2001. A new approach for the morphological segmentation of high-resolution satellite imagery. Geosc. Remote Sens. IEEE Trans. 39 (2), 309–320.
Rasband, W.S., 1997–2014. ImageJ. U. S. National Institutes of Health, Bethesda, Maryland, USA. http://imagej.nih.gov/ij/.
Retornaz, T., 2007. Automatic Detection of Text From Natural Scenes: A Semantic Descriptor for Content Based Image Retrieval. École Nationale Supérieure des Mines de Paris Theses.
Retornaz, T., Marcotegui, B., 2007. Scene text localization based on the ultimate opening. In: Proceedings of the 8th International Symposium on Mathematical Morphology and its Applications to Image and Signal Processing, 1, pp. 177–188.
Salembier, P., Oliveras, A., Garrido, L., 1998. Anti-extensive connected operators for image and sequence processing. IEEE Trans. Image Process. 7 (4), 555–570.
Salembier, P., Serra, J., 1995. Flat zones filtering, connected operators, and filters by reconstruction. IEEE Trans. Image Process. 4, 1153–1160.
Serna, A., Marcotegui, B., Decencière, E., Baldeweck, T., Pena, A.-M., Brizion, S., 2014. Segmentation of elongated objects using attribute profiles and area stability: application to melanocyte segmentation in engineered skin. Pattern Recognit. Lett. 47, 172–182. Advances in Mathematical Morphology.
Serra, J., 1988. Image analysis and mathematical morphology. Theoretical Advances, 2. Academic Press, London.
Serra, J., Vincent, L., 1992. An overview of morphological filtering. Circuits Syst. Signal Process. 11 (1), 47–108.
Silva, A.G., de Alencar Lotufo, R., 2011. Efficient computation of new extinction values from extended component tree. Pattern Recognit. Lett. 32 (1), 79–90.
Soille, P., 2005. Beyond self-duality in morphological image analysis. Image Vis. Comput. 23 (2), 249–257. Discrete Geometry for Computer Imagery.
Urbach, E., Boersma, N., Wilkinson, M., 2005. Vector-attribute filters. In: Ronse, C., Najman, L., Decencière, E. (Eds.), Mathematical Morphology: 40 Years On. In: Computational Imaging and Vision, 30. Springer Netherlands, pp. 95–104.
Urbach, E., Roerdink, J., Wilkinson, M., 2007. Connected shape-size pattern spectra for rotation and scale-invariant classification of gray-scale images. Pattern Anal. Mach. Intell. IEEE Trans. 29 (2), 272–285.
Vachier, C., Meyer, F., 1995. Extinction value: a new measurement of persistence. In: In IEEE Workshop on Nonlinear Signal and Image Processing, pp. 254–257.
Veltkamp, R.C., Hagedoorn, M., 2000. Shape similarity measures, properties, and constructions. In: In Advances in Visual Information Systems, 4th International Conference. Springer, pp. 467–476.
Wilkinson, M.H., Pesaresi, M., Ouzounis, G.K., 2016. An efficient parallel algorithm for multi-scale analysis of connected components in gigapixel images. ISPRS Int. J. Geoinf. 5 (3), 22.
Wilkinson, M.H., Soille, P., Pesaresi, M., Ouzounis, G.K., 2011. Concurrent computation of differential morphological profiles on giga-pixel images. In: International Symposium on Mathematical Morphology and Its Applications to Signal and Image Processing. Springer, pp. 331–342.
Xu, Y., Géraud, T., Najman, L., 2013. Two applications of shape-based morphology: blood vessels segmentation and a generalization of constrained connectivity. In: Mathematical Morphology and Its Applications to Signal and Image Processing. Lecture Notes in Computer Science, 7883. Springer Berlin Heidelberg, pp. 390–401.
Xu, Y., Monasse, P., Géraud, T., Najman, L., 2014. Tree-based morse regions: a topological approach to local feature detection. Image Process. IEEE Trans. 23 (12), 5612–5625.

Please cite this article as: W.A.L. Alves et al., Ultimate levelings, Computer Vision and Image Understanding (2017), http://dx.doi.org/10.1016/j.cviu.2017.06.010